# INFORMATION TO USERS

This manuscript has been reproduced from the microfilm master. UMI films the text directly from the original or copy submitted. Thus, some thesis and dissertation copies are in typewriter face, while others may be from any type of computer printer.

**The quality of this reproduction is dependent upon the quality of the copy submitted.** Broken or indistinct print, colored or poor quality illustrations and photographs, print bleedthrough, substandard margins, and improper alignment can adversely affect reproduction.

In the unlikely event that the author did not send UMI a complete manuscript and there are missing pages, these will be noted. Also, if unauthorized copyright material had to be removed, a note will indicate the deletion.

Oversize materials (e.g., maps, drawings, charts) are reproduced by sectioning the original, beginning at the upper left-hand corner and continuing from left to right in equal sections with small overlaps.

ProQuest Information and Learning
300 North Zeeb Road, Ann Arbor, MI 48106-1346 USA
800-521-0600

**University of Alberta**

# Finite-amplitude development of time-varying abyssal currents

by

Seung Ji Ha 

A thesis submitted to the Faculty of Graduate Studies and Research in partial fulfillment of the requirements for the degree of Master of Science

in

Applied Mathematics

DEPARTMENT of MATHEMATICAL AND STATISTICAL SCIENCES

EDMONTON, ALBERTA

SPRING 2005

## Abstract

A finite amplitude theory is developed for the evolution of marginally unstable modes of time-varying abyssal currents on a sloping bottom. The evolution of this abyssal current is modeled by a geostrophic baroclinic theory of convective destabilization which allows for large-amplitude isopycnal deflection and filters out shear-based barotropic instabilities. Linear stability theory is used to generate a marginal stability curve. There are two different situations to be considered. One is for marginally unstable modes not located at the minimum of the marginal stability curve. An amplitude equation shows that the modes eventually equilibrate with a new finite amplitude periodic solution. The other case corresponds to the modes at the minimum of the marginal stability curve.

**Acknowledgements**

First, I would like to thank my supervisor, Dr. Gordon Swaters. I am deeply indebted to him for the guidance and support he has provided throughout the course of this work. He always encourages me to research and is willing to help me whenever I have troubles. This thesis has not been possible without all his help.

I would also like to thank all my friends in Canada and Korea for encouraging me to finish this thesis. Especially, I am grateful to Eun Ah Lee and Ryan Kusch for helping with the preparation of this thesis.

Finally, I would like to thank my parents and my sister for their love and continued support. This thesis is dedicated to them.

# Contents

# List of Figures

# Chapter 1

# Introduction

When viewed globally, the vertical temperature structure of the ocean can be separated into two distinct zones. The first is an upper, near the surface region, roughly 1 $km$ deep, that is characterized by the temperature sharply decreasing with depth. This upper region is called the "thermocline zone" and its lower boundary is called sometimes simply the "thermocline." Ocean currents in the thermocline zone are principally driven by atmospheric winds and latitudinal variations in solar heating. On the planetary scale, these currents are the dominant mechanism by which the warm waters of the tropics are transported to the polar regions.

Below the thermocline, and extending to the bottom, is the vast volume of cold, dense ocean water (i.e., between $0°C$ and $2°C$ and some 3 to 4 $km$ thick), that is called the abyssal zone or region. The abyssal region is characterized by a relatively weak vertical temperature gradient. Abyssal currents tend to be somewhat slower than near-surface currents and are principally driven by deep convection and density contrasts with the surrounding ocean. These deep ocean currents are the dominant mechanism by which cold polar water returns to the

equator (and beyond).

It has long been recognized that the contribution from abyssal currents should be included in the overall heat budget of the oceans (e.g., Wunsch, 1984). In particular, the role of the abyssal ocean in setting the global average ocean temperature is significant. Even though widespread areas of the ocean surface have temperatures on the order of $20°C$ or so, it has been estimated by Worthington (1981), for example, that the impact of the abyssal ocean is to dramatically lower the global average temperature of the ocean to be only about $3.5°C$. In addition, abyssal currents transport salt, and nutrients as well as other chemical and biological components, over great distances.

The water masses of the abyss are created by the cooling of the ocean surface by the atmosphere in the polar regions (Warren, 1981). As the surface waters are cooled, they become more dense and, due to gravity, they sink toward the bottom. The existence of such deep cold water at other latitudes means that there must be a large scale deep circulation, the abyssal circulation, which carries the water formed in the polar regions to the rest of the ocean (Warren, 1981; see, also, Pedlosky, 1996).

The development of a theoretical understanding of the abyssal circulation, its sources, pathways and interaction with the rest of the ocean, has been a challenging problem in physical oceanography. Clearly, there are enormous technological problems associated with collecting oceanographic data, 4 to 5 $km$ deep, from ships located on a rapidly moving ocean surface. Irrespective of the fact that the collection of oceanographic data from the abyss is difficult, the problem of understanding the planetary scale dynamics of the abyssal circulation is one of the central problems in physical oceanography. The abyssal circulation, taken together with the surface circulation, is the means by which incoming solar heating is distributed latitudinally and vertically deep into the ocean. Besides being

an interesting oceanographic problem in its own right, understanding the abyssal circulation is obviously an important component in climate dynamics and variability.

Stommel and Arons (1960) provided the first dynamical explanation for the deep circulation. They showed, based on the Sverdrup vorticity balance, that source-driven abyssal currents on a $\beta$-plane must flow equatorward. However, away from the source region, the Sverdrup vorticity balance does not determine the flow direction. This raises the interesting question concerning determining the dynamical balance(s) that is (are) responsible for maintaining basin scale abyssal flow that is far removed from the source region.

When dense water is formed (e.g., because of atmospheric cooling) it may reach the bottom. If the bottom is sloping, then the combined influences of the Coriolis force and density contrasts may force the current to be transversely constrained and flow with the coastline to its right (left) in the northern (southern) hemisphere. Examples include the Denmark Strait Overflow (DSO, Smith, 1976), the formation and flow of Antarctic Bottom Water (Whitehead and Worthington, 1982), deep water formation in the Adriatic Sea (Zoccolotti and Salusti, 1987), and deep water replacement in the Strait of Georgia (LeBlond *et al.*, 1991 Karsten *et al.*, 1995, Masson, 2002). As shown by Nof (1983), a fully grounded abyssal water mass lying over sloping topography flows, in the fully nonlinear but reduced gravity dynamical limit, nondispersively and steadily in the along slope direction, irrespective of the specific height or vorticity field within the abyssal water mass.

These two dynamical limits (i.e., the Stommel-Arons and the Nof balances) provide a theoretical scenario for the initiation and maintenance of source-driven grounded abyssal flow. That is, in high latitude regions where the deep water is produced (often over sloping topography), the Sverdrup vorticity balance initiates

equatorward flow. Once produced, this water mass can become grounded (i.e., "attached" to the bottom) and geostrophically adjusted, maintaining a Nof-like balance that permits sustained basin scale meridional quasi-steady and coherent abyssal flow. Of course, this picture leaves out many important dynamical processes such as diabatic and planetary effects, baroclinicity, instability, topographic separation and mixing. In addition, such a scenario cannot explain cross-equatorial abyssal currents where the underlying assumptions of geostrophically balanced grounded flow must necessarily break down (see, e.g., Choboter and Swaters, 2003, 2004) or the super-inertial instability process associated with frictional super-critical abyssal overflows (Swaters, 2003).

Swaters (1991) was the first paper to describe the linear baroclinic instability of a grounded abyssal current on a sloping bottom. The instability mechanism modeled by Swaters (1991) is the release of the available gravitational potential energy (AGPE) associated with a relatively dense water mass sitting directly on a sloping bottom surrounded by relatively lighter water. As the abyssal current becomes unstable, down slope propagating plumes develop on the offshore isopycnal incropping. The AGPE is transferred to perturbation potential energy in the overlying water column that is organized into topographic Rossby waves. Jiang and Garwood (1996), Jungclaus *et al.* (2001), Etling *et al.* (2000), and others, have concluded that the instabilities observed in three-dimensional numerical simulations of overflows on a continental slope arise due to the Swaters (1991) instability mechanism.

Subsequently, Swaters (1993) showed that the Swaters (1991) model was an infinite dimensional non-canonical Hamiltonian system and that it was possible to derive Arnol'd-like nonlinear stability conditions. Karsten and Swaters (1996) extended the Swaters (1993) analysis to allow for more realistic topographic configurations.

Notwithstanding the success of the linear instability theory, if the model is to correctly describe the observed transition of an unstable abyssal current to a new equilibrium configuration that continues to allow sustained basin scale abyssal flow, it was necessary to understand the predictions of the theory in the nonlinear regime. Mooney and Swaters (1996) developed a finite amplitude instability theory for the Swaters (1991) model. They showed that it was possible for the instabilities to saturate and for the unstable abyssal current to evolve toward a new quasi-equilibrium state or to form isolated coherent abyssal domes. Swaters (1998) presented numerical simulations based on the Swaters (1991) model and showed that predictions of the weakly nonlinear Mooney and Swaters (1996) theory remained true even in the fully nonlinear regime.

Poulin and Swaters (1999a,b,c) extended the Swaters (1991) model to the case where the overlying water column is continuously stratified. Subsequently, Reszka, Swaters and Sutherland (2002) developed the linear instability theory for this new model and presented numerical simulations for the nonlinear evolution of source driven abyssal flows for parameter values characteristic of the DSO. In addition to showing how this model could reproduce the spatial and temporal characteristics of the mesoscale variability observed in the DSO, these simulations were also able to reproduce the formation of surface intensified eddies that have been observed in satellite imagery of the DSO (Bruce, 1995).

All of the above instability for abyssal currents has been based on assuming the underlying flow is steady. However, recent work on the baroclinic instability of time varying flow has suggested that time dependence can have a profound effect on the stability properties of ocean currents. For example, Pedlosky and Thomson (2003), in a study of the two-layer Phillips' model of baroclinic instability of a zonal flow on a $\beta$-plane (Pedlosky, 1987), have shown that simple time variations in the zonal current can destabilize the flow even if the time average of the

current is itself stable (and vice-versa). Such time dependence occurs on many different time scales and for many different reasons. Some of these reasons include (daily) tidally-forced flow variations, (weekly) weather system induced variability, seasonal variations or even longer time scale interannual variability. In the context of source driven abyssal flow it is easy to imagine that there are seasonal variations in the intensity of the atmospheric cooling which produces the deep convection and this, in turn, will result in a time varying abyssal current.

The principal purpose of this thesis is to develop a weakly nonlinear theory for a marginally unstable, time-varying abyssal current. We point out that Pavec, Carton and Swaters (2004) have recently extended, following the ideas in Pedlosky and Thomson (2003), the *linear* stability theory of Swaters (1991) to the case of a marginally unstable unsteady abyssal flow having an oscillatory component. Our contribution here is to extend the weakly nonlinear instability analysis of Mooney and Swaters (1996) to marginally unstable, time-varying abyssal currents, using the methods described by Pedlosky and Thomson (2003).

That is, we extend the work of Pavec *et al.* (2004) in two important ways. First, we extend the work of Pavec *et al.* (2004) into the nonlinear regime. Second, we develop the theory for the case of a marginally unstable unsteady abyssal flow having an oscillatory component where the underlying corresponds to the "point of marginal stability" (Drazin and Reid, 1981). As we will see the details of these two calculations are dramatically different.

The model for this thesis is the Swaters (1991) equations for abyssal flow. Briefly, this is a two-layer model that is stably stratified with variable bottom topography on an $f$-plane. The model is not completely quasi-geostrophic and the abyssal layer can have a height or thickness field that intersects the bottom (see Fig. 1.1). However, because it is assumed that the thickness of the abyssal layer is small compared to the mean thickness of the overlying water column, the

dynamics of the surrounding ocean is, in fact, quasi-geostrophic, with the potential vorticity (PV) containing relative vorticity, vortex stretching associated with the interface between the abyssal current and the upper layer, and a background PV gradient associated with a sloping bottom.

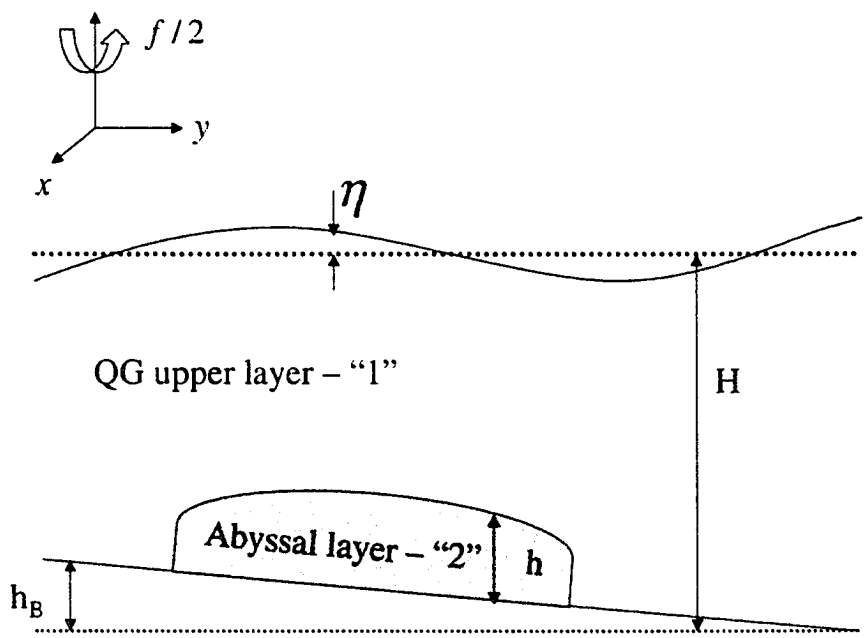


Figure 1.1: Geometry of the model used in this thesis

The outline of this thesis is as follows. In Chapter 2, we derive the Swaters (1991) model in two different ways. First, we derive the equations using the asymptotic methods of Swaters (1991). In addition, we present a derivation

of the model based on the relevant PV equations. Chapter 2 then goes on to describe the general linear, nonlinear and normal mode stability theory for abyssal currents based on the Swaters (1991) model. Several general stability properties are presented including necessary conditions for instability, a semi-circle theorem and a high wavenumber cutoff. Finally, in Chapter 2 the normal stability problem for a constant, or un-sheared, abyssal flow on a sloping bottom is solved and the stability characteristics are described. These properties are essential to the building of the finite amplitude instability theory for time varying flows that is developed in Chapters 3 and 4.

As shown by Mooney and Swaters (1996), and as is well known in the nonlinear theory of baroclinic instability in the context of the Phillips' model (Pedlosky, 1970, 1972, 1982a,b, 1987), the mathematical details of the development of the weakly nonlinear theory depend crucially on the underlying perturbation mode being examined. Chapter 3 develops the weakly nonlinear instability theory for a time varying abyssal flow, when the marginally unstable mode *does not* correspond to the "point of marginal stability." In this situation, at each stage of the asymptotic expansion, the governing partial differential equations are linear so that higher harmonics are generated only as a second order effect.

In Chapter 3, we derive and analyze the nonlinear governing equation for the modal amplitude when the background flow is a time periodic function. The Mooney and Swaters (1996) solution is reviewed. We show that in the finite amplitude limit, the normal mode amplitude, when the abyssal flow is periodic in time, must satisfy a *nonlinear Mathieu equation*. Two situations involving a time periodic abyssal flow are considered in some detail in Chapter 3.

The first situation corresponds to when the normal mode is slightly unstable, i.e., the abyssal current is slightly supercritical. We show that even when the nonlinear terms are neglected in the (normal mode) amplitude equation there

exist periodic, with respect to time, abyssal flow configurations that can stabilize what is, in the time averaged sense, nevertheless an unstable abyssal flow. However, this situation only occurs for a relatively small set of flow parameters. Generically, when the underlying abyssal flow is already marginally unstable, we show that periodic time variability is not a stabilizing influence. However, the presence of the nonlinear terms in the amplitude equation ultimately always leads to the amplitude oscillating in time.

We investigate the role of periodic time variability in a marginally unstable abyssal flow by numerically integrating the amplitude equation. In particular, we describe the evolution of the normal mode amplitude when the period of the time varying part of the abyssal flow is short, comparable, and long, and when the magnitude of the time varying part of the abyssal flow is small, comparable, and large, respectively, compared to the solution of the amplitude equation when time variability is not present (i.e., the Mooney and Swaters (1996) solution). Generally speaking, for the low frequency variability, the normal mode amplitude still evolves periodically although the temporal structure is complex. For the higher frequency time variability, the normal mode amplitude continues to oscillate in time, and appears to be globally bounded, but the oscillations are no longer periodic at a single frequency.

The second situation corresponds to when the normal mode is slightly stable, i.e., the abyssal current is slightly subcritical. We show that when the nonlinear terms are neglected in the (normal mode) amplitude equation there exist time periodic abyssal flow configurations that can destabilize what is, in the time averaged sense, nevertheless a stable abyssal flow and that this is the generic situation. However, the presence of the nonlinear terms in the amplitude equation ultimately always leads to the amplitude oscillating in time. We present a numerical simulation that illustrates this property.

In Chapter 4, we develop the weakly nonlinear instability theory for time varying abyssal flows when the marginally unstable mode *does* correspond to the "point of marginal stability." In many ways, this is the real nonlinear stability problem. But this analysis is complicated by the fact that, even at lowest order, the unstable mode is governed by a fully nonlinear partial differential equation (this was first shown for the Phillips' model for the baroclinic instability of a steady zonal flow by Pedlosky, 1982a,b, and later was more completely discussed by Warn and Gauthier, 1989).

This means that, even at lowest order, there are an infinity of harmonics produced. Following the solution procedure of Mooney and Swaters (1996), we introduce a spectral decomposition technique that leads to an infinite set of coupled nonlinear partial differential equations that will describe the spatial and temporal evolution of the modal amplitudes.

If the infinite set of modal amplitude equations is truncated, on a purely *ad hoc* basis, to include only the fundamental mode and the mean flow it generates, then the resulting set of equations can be shown to be equivalent to the sine-Gordon equation with time-dependent forcing. This was first shown for the Phillips' model for the baroclinic instability of a steady flow by Gibbon *et al.* (1979) and for the abyssal flow problem by Mooney and Swaters (1996). Unfortunately, we have not been able to find exact solutions to our truncated model equations for a time varying mean flow. However, Mooney and Swaters (1996) have shown that, without the forcing terms associated with the time dependent abyssal current, the truncated model has a soliton solution that can be identified as a steadily-travelling coherent abyssal dome. We derive transport equations, by introducing a nonlinear *WKB* technique, describing the evolution of the soliton solution of the truncated model assuming that the time variation of the underlying abyssal current is slow compared to the advective time scale associated with the soliton.

Finally, in Chapter 5, there is a discussion of the results, concluding remarks, and suggestions for further research.

# Chapter 2

# Derivation of the governing equations

Geophysical fluids are characterized by a striking difference between the length scale of the vertical motion compared to that of the horizontal motion. In the atmosphere, for example, the vertical movement of air associated with typical weather system takes place almost entirely in the region between the surface of the earth and the tropopause, a distance of, on average, about 10 $km$. Coherent horizontal movement in the atmosphere occurs on a much vaster scale; a typical wavelength for a series of disturbances organized as planetary Rossby waves may be 1000 to 2000 $kms$, or more. In the ocean, the depth of the mid-ocean is about 5 $km$, and the dynamical horizontal length scale is about 100 $km$. We may take advantage of these scale differences by developing a theory which, to leading order, ignores vertical accelerations compared to horizontal accelerations. The resulting equations are the *shallow water equations*. In this thesis, we use a two layer system of shallow water equations (see Fig. 1) as the starting point for the

development of our baroclinic model for abyssal currents.

The outline of this Chapter is as follows. In Section 2.1, we derive the shallow water equations for each layer in our model based on a scaling argument applied to the inviscid, incompressible Navier-Stokes equations with constant density. In Section 2.2, we develop scalings to highlight the dynamics we expect to occur in the specific physical situation studied here. In Section 2.3 we derive the Swaters (1991) model as a systematic asymptotic reduction of the nondimensional two layer shallow water equations derived in Section 2.2. In Section 2.4, we present an alternative derivation of the model equations based on the potential vorticity formulation of the two layer shallow water equations. In Section 2.5, we review, based on the theory in Swaters (1991), the known linear stability characteristics for general steady abyssal flow solutions to the model including necessary conditions for instability, a high wave number cutoff and a semi-circle theorem. In addition, the general form of the linear and nonlinear stability equations is derived. In Section 2.6, we describe the steady abyssal current solutions that we will use to develop the theory in this thesis and present some specific stability results for this flow configuration.

## 2.1 The two-layer shallow water equations

We begin our derivation of the model equations by first deriving the shallow water equations from the inviscid incompressible Navier-Stokes equations with constant density for a single layer of fluid. Once this is done, it will be straightforward to see how the two layer model can be obtained. We also remark that our derivation will assume $f$-plane dynamics so that the latitudinal variation of the Coriolis parameter is neglected.

The Navier-Stokes equations for an inviscid, incompressible fluid with constant

density, in the presence of gravity, can be written in the form

$$\mathbf{u}_t + (\mathbf{u}\cdot\nabla)\mathbf{u} + f(\hat{\mathbf{e}}_3 \times \mathbf{u}) = -\frac{1}{\rho}\nabla p - g\hat{\mathbf{e}}_3, \tag{2.1.1}$$

$$\nabla \cdot \mathbf{u} = 0, \tag{2.1.2}$$

where $\mathbf{u}(x, y, z, t) = (u, v, w)$ where $u, v$, and $w$ are the along slope, across slope, and vertical velocities, respectively, $\rho$ is the constant density, $p(x, y, z, t)$ is the total pressure, $\nabla = (\partial_x, \partial_y, \partial_z)$, and $f = 2\Omega\sin(\theta_0)$ where $\Omega$ is the magnitude of the earth's rotation vector ($\Omega = 2\pi\ radians/day$) and $\theta_0$ is the reference latitude for the $f$-plane approximation (Pedlosky, 1987), $g = 9.8\ m/s^2$ is the gravitational constant, and $\hat{\mathbf{e}}_3$ is the unit basis vector in the positive $z$-direction. Equations (2.1.1) and (2.1.2) are in vector form. It is more convenient to write (2.1.1) and (2.1.2) in the component form

$$u_t + uu_x + vu_y + wu_z - fv = -\frac{1}{\rho}p_x, \tag{2.1.3}$$

$$v_t + uv_x + vv_y + wv_z + fu = -\frac{1}{\rho}p_y, \tag{2.1.4}$$

$$w_t + uw_x + vw_y + ww_z = -\frac{1}{\rho}p_z - g, \tag{2.1.5}$$

$$u_x + v_y + w_z = 0. \tag{2.1.6}$$

The derivation of the shallow water equations is facilitated by introducing appropriate scalings for the various variables. Let $H$ and $L$ be the horizontal and vertical length scales, respectively. The aspect ratio, denoted as $A_r$, given by

$$A_r = H/L << 1, \tag{2.1.7}$$

for the geophysical flows we are interested in.

If the horizontal velocities are scaled by $U$ and the vertical velocity by $W$, then the continuity equation, (2.1.6), scales like

$$\begin{array}{ccccccc} u_x & + & v_y & + & w_z & = & 0. \\ \frac{U}{L} & & \frac{U}{L} & & \frac{W}{H} & & \end{array}$$

Assuming that $w_z$ scales like $u_x$ and $v_y$, implies that

$$W = \frac{UH}{L} = A_r U.$$

When we scale the vertical momentum equation, (2.1.5), we obtain

$$\begin{array}{ccccccccc} w_t & + & uw_x & + & vw_y & + & ww_z & = & -\frac{1}{\rho}p_z - g, \\ \frac{W}{T} & & \frac{UW}{L} & & \frac{UW}{L} & & \frac{WW}{H} & & \end{array}$$

where we have introduced the time scale $T$. If we use the so called advective time scale assumption $T = L/U$ and substitute in the above relation for $W$, we find that all the terms on the left hand side of (2.1.5), i.e., the vertical acceleration terms, are $O(A_r U^2/L)$. Now, typical mid ocean scales are about (LeBlond and Mysak, 1978, Gill, 1982, Pedlosky, 1987, Mellor, 1996)

$$U = 10^{-1} m/s,\ L = 10^5 m,\ A_r = 10^{-2}\ \ (H \simeq 5\ km)$$

$$\Longrightarrow A_r U^2/L \simeq O(10^{-9}\ m/s^2). \tag{2.1.8}$$

Since $g \simeq 10\ m/s^2$, clearly, the vertical acceleration terms are insignificant compared to the gravitational term in the vertical momentum equation. It follows that the only term that can balance $g$ must be the pressure gradient term, which implies that to a significant approximation, the vertical momentum equation reduces to

$$\frac{1}{\rho}p_z = -g. \tag{2.1.9}$$

Integrating this equation with respect to $z$ leads to

$$p(x, y, z, t) = -\rho g z + \phi(x, y, t), \tag{2.1.10}$$

where $\phi$ is a "constant" of integration. Note that $\phi$ is independent of $z$. It follows that $p_{x,y} = \phi_{x,y}$ so that the pressure gradient terms in the horizontal momentum equations are independent of $z$. Thus, if $(u, v)$ are initially independent of $z$,

it follows that it is consistent to suppose that they will remain so subsequently. That is, we assume $u_z = v_z = 0$ for all $t \geq 0$.

We now consider a two layer configuration where each layer has a different density. For convenience, we denote the upper layer (i.e., the overlying ocean) as layer one, and the lower layer (i.e., the abyssal layer), as layer two and subscript, where necessary, the various variables with a "1" or a "2" to denote the respective layer.

Thus, the upper layer pressure will be of the form

$$p_1(x, y, z, t) = -\rho_1 g z + \phi_1(x, y, t). \tag{2.1.11}$$

If we denote the position of the free surface associated with the upper layer to be given by $z = \eta(x, y, t)$ and that the pressure on the free surface is constant (which we can take to be zero), it follows that the dynamic boundary condition is given by

$$0 = -\rho_1 g \eta(x, y, t) + \phi_1(x, y, t), \tag{2.1.12}$$

which determines $\phi_1(x, y, t)$. Thus $p_1$ is determined by combining (2.1.11) and (2.1.12), to give,

$$p_1(x, y, z, t) = -\rho_1 g z + \rho_1 g \eta. \tag{2.1.13}$$

To determine $p_2$, it is convenient to write the analogue of (2.1.11) in the form

$$p_2(x, y, z, t) = \rho_1 g H - \rho_2 g(z + H) + \phi_2(x, y, t). \tag{2.1.14}$$

The dynamic boundary condition on the interface between the abyssal layer and overlying fluid, located at $z = -H - sy + h$ (see Fig. 1), is that the total pressure must be continuous across the interface, i.e.,

$$p_1(x, y, -H - sy + h, t) = p_2(x, y, -H - sy + h, t). \tag{2.1.15}$$

It follows from (2.1.15), (2.1.13) and (2.1.14) that,

$$\rho_1 g(\eta + H + sy - h) = \rho_1 g H - \rho_2 g(-H - sy + h + H) + \phi_2, \tag{2.1.16}$$

which can be re-arranged into the form

$$\phi_2 = \rho_1 g\eta + \rho_2 g'(h - sy), \tag{2.1.17}$$

where $g' = g(\rho_2 - \rho_1)/\rho_2 > 0$ is called the reduced gravity. Substituting (2.1.17) into (2.1.14), we see that

$$p_2 = \rho_1 g(H + \eta) - \rho_2(z + H) + \rho_2 g'(h - sy). \tag{2.1.18}$$

We now develop the appropriate kinematic boundary conditions for the upper layer. For notational convenience we delete the "1" subscript for the moment. As mentioned above, the position of the ocean surface is given by $z = \eta(x, y, t)$. It follows that

$$\frac{D}{Dt}(z - \eta) = 0 \text{ on } z = \eta(x, y, t), \tag{2.1.19}$$

where the *total time derivative* $D/Dt$ is given by

$$\frac{D}{Dt} = \frac{\partial}{\partial t} + \mathbf{u} \cdot \nabla = \frac{\partial}{\partial t} + u\frac{\partial}{\partial x} + v\frac{\partial}{\partial y} + w\frac{\partial}{\partial z}.$$

So, (2.1.19) can be expressed as

$$(\partial_t + u\partial_x + v\partial_y + w\partial_z)(z - \eta) = 0 \text{ on } z = \eta(x, y, t),$$

from which it follows that

$$w = \eta_t + u\eta_x + v\eta_y = \frac{D_H \eta}{Dt} \text{ on } z = \eta(x, y, t),$$

where $D_H/Dt$ is the *total "horizontal" time derivative* given by

$$\frac{D_H}{Dt} = \frac{\partial}{\partial t} + \mathbf{u}_H \cdot \nabla_H = \frac{\partial}{\partial t} + u\frac{\partial}{\partial x} + v\frac{\partial}{\partial y},$$

where $\mathbf{u}_H = (u, v)$ and $\nabla_H = (\partial_x, \partial_y)$.

It therefore follows, re-introducing the "1" subscript, that

$$w_1 = \eta_t + u_1\eta_x + v_1\eta_y \text{ on } z = \eta(x, y, t), \tag{2.1.20}$$

and, similarly, on the interface between the abyssal layer and overlying ocean, located at $z = -H - sy + h$, that

$$w_1 = (\partial_t + u_1\partial_x + v_1\partial_y)(h - sy) \text{ on } z = -H - sy + h. \tag{2.1.21}$$

We now turn to writing the continuity equation (2.1.6) in a more convenient form for the upper layer. To begin, we integrate (2.1.6) vertically over the entire upper layer water column, i.e.,

$$\int_{-H-sy+h}^{\eta} u_{1x} + v_{1y} + w_{1z}\ dz = 0.$$

This gives us

$$w_1(x, y, \eta, t) - w_1(x, y, -H - sy + h, t) = -(\eta + H + sy - h)(u_{1x} + v_{1y}). \tag{2.1.22}$$

If (2.1.20) and (2.1.21) are substituted into (2.1.22), we obtain

$$\frac{D_H(\eta + H + sy - h)}{Dt} + (\eta + H + sy - h)(u_{1x} + v_{1y}) = 0, \tag{2.1.23}$$

which can be re-arranged into

$$(\eta + sy - h)_t + \mathbf{u}_{H1} \cdot \nabla_H(\eta + sy - h) + (\eta + H + sy - h)\nabla_H \cdot \mathbf{u}_{H1}, \tag{2.1.24}$$

and further into the form

$$(\eta - h)_t + \nabla_H \cdot [\mathbf{u}_{H1}(\eta + H + sy - h)] = 0, \tag{2.1.25}$$

where we have used the vector identity

$$\nabla \cdot (\mathbf{b}a) = a\nabla \cdot \mathbf{b} + \mathbf{b} \cdot \nabla a, \tag{2.1.26}$$

for an arbitrary scalar function $a(\mathbf{x})$ and vector function $\mathbf{b}(\mathbf{x})$.

The development of the kinematic boundary conditions for the lower layer follows in exactly the same manner. For the abyssal layer, the "upper boundary"

is the interface between the abyssal layer and the overlying ocean (located at $z = -H - sy + h$) and the "lower boundary" is the ocean bottom (located at $z = -H - sy$). Thus, we find that

$$w_2 = \frac{D_H}{Dt}(-H - sy + h) \text{ on } z = -H - sy + h, \tag{2.1.27}$$

$$w_2 = \frac{D_H}{Dt}(-H - sy) \text{ on } z = -H - sy. \tag{2.1.28}$$

Hence, if we vertically integrate the continuity equation (2.1.6) over the lower layer thickness, i.e.,

$$\int_{-H-sy}^{-H-sy+h} u_{2x} + v_{2y} + w_{2z} \; dz = 0, \tag{2.1.29}$$

it follows that

$$w_2(x, y, -H - sy + h, t) - w_2(x, y, -H - sy, t) + (u_{2x} + v_{2y})h = 0. \tag{2.1.30}$$

If (2.1.27) and (2.1.28) are substituted into (2.1.30), we obtain

$$\frac{D_H}{Dt}(-H - sy + h) - \frac{D_H}{Dt}(-H - sy) + (u_{2x} + v_{2y})h = 0, \tag{2.1.31}$$

which simplifies to

$$\frac{D_H h}{Dt} + (u_{2x} + v_{2y})h = 0, \tag{2.1.32}$$

or, equivalently,

$$h_t + \nabla_H \cdot (\mathbf{u}_{2H} h) = 0. \tag{2.1.33}$$

We summarize our work so far. Because we need to nondimensionalize the two layer shallow water equations and then subsequently introduce an asymptotic expansion we will now introduce asterisks into the equations so that variables with asterisks are to be considered dimensional. Also, we will delete the $H$ subscript from the gradient and the velocity fields since henceforth we will only work with the horizontal gradient and velocity fields, respectively.

Thus, from (2.1.1) and (2.1.26), the upper layer equations are given by

$$\mathbf{u}_{1t^*}^* + (\mathbf{u}_1^* \cdot \nabla^*)\mathbf{u}_1^* + f(\widehat{\mathbf{e}}_3 \times \mathbf{u}_1^*) + g\nabla^*\eta^* = 0, \tag{2.1.34}$$

$$(\eta^* - h^*)_{t^*} + \nabla^* \cdot [\mathbf{u}_1^*(\eta^* + H + s^*y^* - h^*)] = 0, \tag{2.1.35}$$

where we recall that

$$\frac{1}{\rho_1}\nabla^* p_1^* = g\nabla^*\eta^*.$$

The lower layer equations are given by

$$\mathbf{u}_{2t^*}^* + (\mathbf{u}_2^* \cdot \nabla^*)\mathbf{u}_2^* + f(\widehat{\mathbf{e}}_3 \times \mathbf{u}_2^*) + \frac{1}{\rho_2}\nabla^* p_2^* = 0, \tag{2.1.36}$$

$$h_{t^*}^* + \nabla^* \cdot [\mathbf{u}_2^* h^*] = 0, \tag{2.1.37}$$

with pressure continuity across the interface given by

$$p_2^* = \rho_1 g\eta^* + \rho_2 g'(h^* - s^*y^*). \tag{2.1.38}$$

## 2.2 Scalings for the two layer shallow water equations

We now scale the two layer shallow water equations to obtain the Swaters (1991) baroclinic abyssal current model. We will introduce variables without an asterisk and these are henceforth all non-dimensional. The horizontal length is the internal deformation associated with the overlying ocean, not the abyssal layer. This is the appropriate length scale if potential vorticity (PV) variations associated with deformations of the interface between the two layers is to be the same order of magnitude as the relative vorticity in the upper layer (Swaters, 1991). That is,

$$(x^*, y^*) = L^*(x, y) = \frac{(g'H)^{\frac{1}{2}}}{f}(x, y), \tag{2.2.1}$$

where $L^* = (g'H)^{\frac{1}{2}}/f$ is the internal radius of deformation of the upper layer (Pedlosky, 1987). Note that $(g'H)^{\frac{1}{2}}$ is the phase speed of a long internal gravity wave unaffected by rotation (Pedlosky, 1987).

Second, we introduce the advective time scaling,

$$t^* = (fL^*/s^*g')t. \tag{2.2.2}$$

We note that $s^*g'/f$ is the *Nof speed*, which is the speed at which an isolated abyssal eddy travels along a bottom with constant slope $s^*$ assuming that there is no baroclinic interaction with the surrounding fluid (Nof, 1983). The Nof speed will form the velocity scaling for the abyssal layer.

Third, the abyssal layer height is scaled as

$$h^* = s^*L^*h. \tag{2.2.3}$$

where $s^*$ is the slope of the bottom topography. More generally, $s^*$ can be regarded as a typical value for the bottom slope and thus $s^*L^*$ will be a characteristic bottom variation in the height of the topography over an internal deformation radius.

Fourth, the upper layer velocity and variations in the height of the ocean surface are scaled as follows

$$\mathbf{u}_1^* = \frac{s^*g'}{f}\mathbf{u}_1, \tag{2.2.4}$$

$$\eta^* = \frac{s^*g'L^*}{g}\eta. \tag{2.2.5}$$

These scalings may seem a little unusual at first glance. Note that we have scaled the upper layer velocity field by the Nof velocity. However, as shown by Swaters (1991), this is the correct scaling to use if the relative vorticity is to scale similar to the potential vorticity changes induced by the abyssal layer height, i.e.,

$$O\left(\nabla^* \times \mathbf{u}_1^*\right) \simeq O\left(fh^*/H\right) \Longrightarrow \mathbf{u}_1^* \simeq O\left(s^*g'/f\right).$$

The scaling for $\eta^*$ is constructed so that $\mathbf{u}_1^*$ and $\eta^*$ are in geostrophic balance to leading order. That is, to leading order, we assume that the horizontal pressure gradient scales like the Coriolis terms.

Fifth, the velocity and pressure fields in the abyssal current are assumed to be in geostrophic balance, to leading order, and as mentioned earlier, the abyssal velocity is scaled by the Nof velocity. That is,

$$\mathbf{u}_2^* = \frac{g's^*}{f}\mathbf{u}_2, \tag{2.2.6}$$

$$p_2^* = \rho_2 L^* g' s^* p_2. \tag{2.2.7}$$

These are the basic scalings for the dimensional model. We now substitute these definitions, so to speak, into the dimensional shallow water equations and obtain the nondimensional equations. When one does that, there will be a single nondimensional parameter, denoted as $s$, and related to the bottom slope parameter $s^*$, via the relation

$$s = \frac{s^* L^*}{H}. \tag{2.2.8}$$

This relationship can be rewritten as

$$s = \frac{s^* g'/f}{\sqrt{g'H}}, \tag{2.2.9}$$

which allows us to interpret the parameter $s$ as the ratio of the Nof speed to the speed of long baroclinic gravity waves. A small $s$ acts as a low band pass filter to remove the long gravity waves and to focus attention on baroclinic sub-inertial processes (Swaters and Flierl, 1991).

Finally, we comment on what typical values for the scalings would correspond to abyssal currents. Typical values for the dimensional parameters appropriate for a continental shelf (see Swaters and Flierl, 1991) are $h^* \approx 40$ $m$, $H \approx 250$ $m$, $L^* \approx 15$ $km$, $t^* \approx 7$ $days$ which implies a Nof velocity of about 3 $cm/s$. For deeper basin scale abyssal flows, such as the DSO, typical values would be about

$h^* \approx 100\ m$, $H \approx 4000\ m$, $L^* \approx 15\ km$, $t^* \approx 7\ days$ which implies a Nof velocity, again, of about 3 $cm/s$ (see Reszka *et al.*, 2002). Typical bottom slopes are on the order of $s^* \approx 10^{-2}$ which suggests that $s \approx 10^{-1}$ to $10^{-2}$.

The *dimensional* momentum equation for the upper layer is given by (2.1.34). If the above scalings are introduced into this equation, one gets the following *non-dimensional* momentum equation

$$\frac{s(g'H)^{\frac{1}{2}}}{\frac{(g'H)^{\frac{1}{2}}}{g'} \cdot \frac{g'}{(g'H)^{\frac{1}{2}} fs}} \mathbf{u}_{1t} + s(g'H)^{\frac{1}{2}} \frac{f}{(g'H)^{\frac{1}{2}}} (\mathbf{u}_1 \cdot \nabla) s(g'H)^{\frac{1}{2}} \mathbf{u}_1$$

$$+ f(\widehat{\mathbf{e}}_3 \times (g'H)^{\frac{1}{2}} s\mathbf{u}_1) + \frac{gf}{(g'H)^{\frac{1}{2}}} \nabla \frac{sHg'}{g} \eta = 0, \tag{2.2.10}$$

which can be simplified to

$$s(g'H)^{\frac{1}{2}} fs\mathbf{u}_{1t} + s^2 (g'H)^{\frac{1}{2}} f(\mathbf{u}_1 \cdot \nabla)\mathbf{u}_1$$

$$+ f(g'H)^{\frac{1}{2}} s(\widehat{\mathbf{e}}_3 \times \mathbf{u}_1) + \frac{fsHg'}{(g'H)^{\frac{1}{2}}} \nabla \eta = 0, \tag{2.2.11}$$

and yet further to

$$s\mathbf{u}_{1t} + s(\mathbf{u}_1 \cdot \nabla)\mathbf{u}_1 + \widehat{\mathbf{e}}_3 \times \mathbf{u}_1 + \nabla \eta = 0. \tag{2.2.12}$$

Applying the above scalings to the dimensional continuity equation for the upper layer, (2.1.35), yields the following *non-dimensional* continuity equation for the upper layer

$$\frac{(\frac{sHg'}{g}\eta - sHh)_t}{\frac{(g'H)^{\frac{1}{2}}}{g'} \frac{g'}{(g'H)^{\frac{1}{2}} fs}} + \frac{f}{(g'H)^{\frac{1}{2}}} \nabla \cdot [s(g'H)^{\frac{1}{2}} \mathbf{u}_1 (\frac{sHg'}{g}\eta + H$$

$$+ \frac{(g'H)^{\frac{1}{2}} sf}{g'} \cdot \frac{(g'H)^{\frac{1}{2}}}{f} sy - sHh)] = 0, \tag{2.2.13}$$

which can be simplified to

$$fs(\frac{sHg'}{g}\eta - sHh)_t + sf\nabla \cdot [\mathbf{u}_1 (\frac{sHg'}{g}\eta + H + Hsy - sHh)] = 0. \tag{2.2.14}$$

The stratification characteristics of abyssal ocean currents has

$$0 < g'/g = (\rho_2 - \rho_1)/\rho_2 << 1,$$

which allows us to neglect the free surface terms of order $O(g'/g)$ in the upper layer continuity equation (Swaters and Flierl, 1991). This is equivalent to assuming that the ocean surface is a rigid lid (Swaters, 1991). Making this assumption implies that

$$-Hfsh_t + sf\nabla \cdot [\mathbf{u}_1(H + Hsy - sHh)] = 0, \tag{2.2.15}$$

which can be simplified to

$$sh_t + \nabla \cdot [\mathbf{u}_1(sh - sy - 1)] = 0. \tag{2.2.16}$$

The non-dimensional equations for the lower layer are obtained using exactly the same procedure starting from equations (2.1.36) and (2.1.37), yielding

$$s\mathbf{u}_{2t} + s(\mathbf{u}_2 \cdot \nabla)\mathbf{u}_2 + \widehat{\mathbf{e}}_3 \times \mathbf{u}_2 + \nabla p_2 = 0,$$

$$h_t + \nabla \cdot (h\mathbf{u}_2) = 0.$$

We see immediately that the abyssal layer continuity equation does not have the parameter $s$ in it. That is, all terms are $O(1)$. This is a consequence of the fact that the abyssal height has been scaled to allow finite height variations. It is this property which implies that the lower layer dynamics are not quasigeostrophic.

If we apply the scaling assumptions to the pressure continuity condition (2.1.38), we obtain

$$\frac{\rho_2(g'H)^{\frac{1}{2}}g'(g'H)^{\frac{1}{2}}fs}{fg'}p_2 = \rho_2 g'(sHh - \frac{(g'H)^{\frac{1}{2}}f}{g'} \cdot \frac{(g'H)^{\frac{1}{2}}}{f}sy) + \frac{\rho_1 gsHg'}{g}\eta, \tag{2.2.17}$$

which simplifies to

$$\rho_2 g'Hsp_2 = \rho_2 g'(sHh - Hsy) + \rho_1 sHg'\eta, \tag{2.2.18}$$

and yet further to

$$\rho_2 s p_2 = \rho_2(sh - sy) + \rho_1 s\eta. \tag{2.2.19}$$

If we use the definition of the reduced gravity

$$g' = \frac{g\,(\rho_2 - \rho_1)}{\rho_2} \Longleftrightarrow \frac{\rho_1}{\rho_2} = 1 - \frac{g'}{g},$$

and substitute into the pressure continuity condition and then neglect terms of $O\,(g'/g)$, we obtain simply

$$p_2 = \eta + h - y. \tag{2.2.20}$$

For completeness we obtain the appropriate nondimensional horizontal boundary conditions. The stability theory to be developed will be done in the context of a channel with parallel walls located at $y = 0$ and $y = L$, respectively. Because the fluid is inviscid the appropriate boundary condition is that there is no flux of fluid through the wall, which implies the normal velocity at the wall must be zero. This is expressed mathematically as

$$v_{1,2}(x, 0, t) = v_{1,2}(x, L, t) = 0. \tag{2.2.21}$$

In summary, the nondimensional two layer shallow water equations are given by

$$\widehat{\mathbf{e}}_3 \times \mathbf{u}_1 + \nabla\eta = -s\,(\partial_t + \mathbf{u}_1 \cdot \nabla)\,\mathbf{u}_1, \tag{2.2.22}$$

$$\nabla \cdot \mathbf{u}_1 = sh_t - s\nabla \cdot (y\mathbf{u}_1) + s\nabla \cdot (h\mathbf{u}_1), \tag{2.2.23}$$

$$\widehat{\mathbf{e}}_3 \times \mathbf{u}_2 - \widehat{\mathbf{e}}_2 + \nabla(h + \eta) = -s\,(\partial_t + \mathbf{u}_2 \cdot \nabla)\,\mathbf{u}_2, \tag{2.2.24}$$

$$h_t + \nabla \cdot (h\mathbf{u}_2) = 0, \tag{2.2.25}$$

$$p_2 = \eta + h - y. \tag{2.2.26}$$

Note that the location of the small parameter $s$ in the above equations produces the effect suggested in words earlier, which is that the overlying ocean will follow quasigeostrophic dynamics but the abyssal layer will be geostrophic, but not quasigeostrophic.

## 2.3 Asymptotic reduction of the two layer shallow water equations

The Swaters (1991) model can be obtained by a regular asymptotic reduction of the model equations (2.2.22) through to (2.2.26) in the limit $s \to 0$. To begin, we assume an asymptotic expansion of the form

$$(\eta, \mathbf{u}_1, \mathbf{u}_2, p, h) \sim (\eta, \mathbf{u}_1, \mathbf{u}_2, p, h)^{(0)} + s(\eta, \mathbf{u}_1, \mathbf{u}_2, p, h)^{(1)} + \cdots . \tag{2.3.1}$$

When the asymptotic expansion (2.3.1) is substituted into (2.2.22) through to (2.2.26), and terms with similar powers of $s$ are collected together, one obtains five equations, individually of the generic form

$$\mathcal{L}_0\left((\eta, \mathbf{u}_1, \mathbf{u}_2, p, h)^{(0)}\right) + s\mathcal{L}_1\left((\eta, \mathbf{u}_1, \mathbf{u}_2, p, h)^{(0)}, (\eta, \mathbf{u}_1, \mathbf{u}_2, p, h)^{(1)}\right) + \cdots = 0,$$

where the $\mathcal{L}_n$ $(n = 0, 1, 2, \cdots)$ are partial differential operators acting on their arguments. Since the asymptotic expansion is assumed to hold for arbitrary (but, of course, "small") $s$, it follows (see Bender and Orszag, 1978), since there is no explicit $s$ dependence in each of the $\mathcal{L}_n$ "coefficients," that

$$\mathcal{L}_0\left((\eta, \mathbf{u}_1, \mathbf{u}_2, p, h)^{(0)}\right) = \mathcal{L}_1\left((\eta, \mathbf{u}_1, \mathbf{u}_2, p, h)^{(0)}, (\eta, \mathbf{u}_1, \mathbf{u}_2, p, h)^{(1)}\right) = \cdots = 0.$$

We call the $\mathcal{L}_n = 0$ problem the "$O(s^n)$ problem." One can see how the asymptotic solution is, in principle, constructed. From the $O(s^0 = 1)$ problem one determines, in principle, $(\eta, \mathbf{u}_1, \mathbf{u}_2, p, h)^{(0)}$ and from the $O(s)$ problem one determines $(\eta, \mathbf{u}_1, \mathbf{u}_2, p, h)^{(1)}$, and so on, until as many terms in the asymptotic expansion as are wanted are determined. Of course, in practice, the solution of the individual problems is never entirely straightforward. For example, associated with the "higher order" problems, i.e., the $\mathcal{L}_n = 0$ problems when $n = 1, 2, \cdots$, will be certain mathematical solvability conditions.

The $O(1)$ equations are given by

$$\widehat{\mathbf{e}}_3 \times \mathbf{u}_1^{(0)} = -\nabla\eta^{(0)}, \tag{2.3.2}$$

$$\nabla \cdot \mathbf{u}_1^{(0)} = 0, \tag{2.3.3}$$

$$\widehat{\mathbf{e}}_3 \times \mathbf{u}_2^{(0)} = \widehat{\mathbf{e}}_2 - \nabla(h^{(0)} + \eta^{(0)}), \tag{2.3.4}$$

$$h_t^{(0)} + \nabla \cdot (h^{(0)}\mathbf{u}_2^{(0)}) = 0, \tag{2.3.5}$$

$$p_2^{(0)} = -y + \eta^{(0)} + h^{(0)}, \tag{2.3.6}$$

which implies that the velocities are geostrophically determined and can be written in the form

$$\mathbf{u}_1^{(0)} = \left(u_1^{(0)}, v_1^{(0)}\right) = \widehat{\mathbf{e}}_3 \times \nabla\eta^{(0)} = \left(-\eta_y^{(0)}, \eta_x^{(0)}\right), \tag{2.3.7}$$

$$\mathbf{u}_2^{(0)} = \left(u_2^{(0)}, v_2^{(0)}\right) = \widehat{\mathbf{e}}_3 \times \nabla p_2^{(0)}$$

$$= \left(-p_{2y}^{(0)},\ p_{2x}^{(0)}\right) = \left(1 - \eta_y^{(0)} - h_y^{(0)},\ \eta_x^{(0)} + h_x^{(0)}\right). \tag{2.3.8}$$

The abyssal layer model equation is obtained by substituting (2.3.8) into (2.3.5) to give

$$h_t^{(0)} + h_x^{(0)} + J\left(\eta^{(0)}, h^{(0)}\right) = 0. \tag{2.3.9}$$

where the Jacobian $J$ operator is defined as

$$J(A, B) \equiv A_x B_y - A_y B_x. \tag{2.3.10}$$

The model equations for the upper layer are somewhat more subtle to obtain. If (2.3.7) is substituted into (2.3.3) one sees that (2.3.3) will be trivially satisfied for all $\eta^{(0)}$. In other words, the $O(1)$ problem for the upper layer is not closed since there are an insufficient number of equations to determine the leading order solution. In the context of the problem examined here, this is called "geostrophic degeneracy." To fully determine the $O(1)$ solution, it is necessary to examine the

$O(s)$ problem for the upper layer and derive a solvability condition on $\eta^{(0)}$ that will "close" the problem.

The $O(s)$ equation for the upper layer is given by

$$\widehat{\mathbf{e}}_3 \times \mathbf{u}_1^{(1)} + \nabla\eta^{(1)} = -\left(\partial_t + \mathbf{u}_1^{(0)} \cdot \nabla\right) \mathbf{u}_1^{(0)}, \tag{2.3.11}$$

$$\nabla \cdot \mathbf{u}_1^{(1)} = h_t^{(0)} - \nabla \cdot (y\mathbf{u}_1^{(0)}) + \nabla \cdot (h^{(0)}\mathbf{u}_1^{(0)}). \tag{2.3.12}$$

If we form $\nabla \times$ (2.3.11) and substitute in (2.3.7), we obtain

$$\triangle\eta_t^{(0)} + J\left(\eta^{(0)},\ \triangle\eta^{(0)}\right) = -\nabla \cdot \mathbf{u}_1^{(1)}, \tag{2.3.13}$$

where $\triangle = \nabla^2 = \partial_{xx} + \partial_{yy}$.

Finally, if (2.3.12) is used to eliminate $\nabla \cdot \mathbf{u}_1^{(1)}$ in (2.3.13), with (2.3.7) being used again, we get

$$\left(\triangle\eta^{(0)} + h^{(0)}\right)_t + J\left(\eta^{(0)},\ \triangle\eta^{(0)} + h^{(0)} - y\right) = 0. \tag{2.3.14}$$

Equation (2.3.14) is the quasigeostrophic (QG) potential vorticity equation for the upper layer. It "says" that the upper layer QG potential vorticity, given by $\triangle\eta^{(0)} + h^{(0)} - y$, is conserved following the leading order (geostrophic) motion.

The upper layer potential vorticity is comprised of three terms. The first is the relative vorticity term $\nabla \times \mathbf{u}_1^{(0)} = \triangle\eta^{(0)}$, the second is the baroclinic stretching term associated with the height of the abyssal layer $h^{(0)}$, and the third is the background vorticity gradient associated with the sloping bottom, i.e., the $-y$ term.

The Swaters (1991) model therefore corresponds to the set of coupled nonlinear partial differential equations (2.3.9) and (2.3.14), which is to be supplemented by appropriate initial and boundary conditions. Although it is not immediately obvious, in fact (2.3.9) is also the leading potential vorticity equation for the abyssal layer. In the next section we show this by re-deriving the Swaters (1991) model by working from the potential vorticity equations for the full two layer shallow water equations.

## 2.4 Derivation based on a potential vorticity formulation

We are going to convert the two layer shallow water equations into a single potential vorticity equation for each layer. We first take the curl of the momentum equation to derive the vorticity equation, and from this we will find the potential vorticity equation. Dynamically, the potential vorticity has a very important property. In the inviscid limit that is examined here, the potential vorticity is conserved following the motion (Pedlosky, 1987), i.e., it is a Lagrangian invariant.

First, let's consider the upper layer equations. To compute the curl of the upper layer momentum equations we first compute $\partial/\partial_y[\widehat{\mathbf{e}}_1 \cdot (2.2.22)]$ and $\partial/\partial_x[\widehat{\mathbf{e}}_2 \cdot (2.2.22)]$, yielding, respectively,

$$-v_{1y} + \eta_{1xy} = -su_{1ty} - s(u_{1y}u_{1x} + u_1u_{1xy} + v_{1y}u_{1y} + v_1u_{1yy}), \tag{2.4.1}$$

$$u_{1x} + \eta_{1yx} = -sv_{1tx} - s(u_{1x}v_{1x} + u_1v_{1xx} + v_{1x}v_{1y} + v_1v_{1yx}). \tag{2.4.2}$$

Subtracting (2.4.2) from (2.4.1) gives

$$-(u_{1x} + v_{1y}) = s\zeta_{1t} + s[u_1\zeta_{1x} + v_1\zeta_{1y} + (u_{1x} + v_{1y})\zeta_1], \tag{2.4.3}$$

where

$$\zeta_1 = v_{1x} - u_{1y},$$

is the relative vorticity of the upper layer. Equation (2.4.3) can be rewritten as

$$-(u_{1x} + v_{1y}) = s\frac{D\zeta_1}{Dt} + s(u_{1x} + v_{1y})\zeta_1, \tag{2.4.4}$$

where we have used the nondimensional total derivative, given by

$$\frac{D}{Dt} = \frac{\partial}{\partial t} + u_1\frac{\partial}{\partial x} + v_1\frac{\partial}{\partial y}. \tag{2.4.5}$$

The next step is to work with (2.2.23), in the form

$$sh_t + (sh - sy - 1)\nabla \cdot \mathbf{u}_1 + \mathbf{u}_1 \cdot \nabla(sh - sy - 1) = 0. \tag{2.4.6}$$

and then to solve for the horizontal divergence, i.e.,

$$\nabla \cdot \mathbf{u}_1 = -\frac{sh_t + \mathbf{u}_1 \cdot \nabla(sh - sy - 1)}{sh - sy - 1} = -\frac{D(sh - sy - 1)/Dt}{sh - sy - 1} \tag{2.4.7}$$

If this is substituted into (2.4.4), we get

$$s\frac{D\zeta_1}{Dt} - (1 + s\zeta_1)\left[\frac{D(sh - y - 1)/Dt}{sh - sy - 1}\right] = 0. \tag{2.4.8}$$

which can be re-written in the form

$$\frac{D}{Dt}(1 + s\zeta_1) - \frac{1 + s\zeta_1}{sh - sy - 1}\frac{D}{Dt}(sh - sy - 1) = 0, \tag{2.4.9}$$

and, thus, we find

$$\frac{D}{Dt}\left(\frac{1 + s\zeta_1}{1 + sy - sh}\right) = 0. \tag{2.4.10}$$

Equation (2.4.10) is the potential vorticity equation for the upper layer. The nondimensional potential vorticity for the upper layer, here denoted by $PV_1$, is given by

$$PV_1 = \frac{1 + s\zeta_1}{1 + sy - sh}, \tag{2.4.11}$$

and is conserved following the motion.

It is interesting to notice that we can also derive (2.4.10) by scaling the dimensional potential vorticity equation, given generically for the shallow water equations for a single layer, by (see, e.g., Pedlosky, 1987)

$$\frac{D}{Dt^*}\left[\frac{\nabla^* \times \mathbf{u}^* + f}{H_{\text{total}}}\right] = 0, \tag{2.4.12}$$

where $H_{\text{total}}$ is the total layer thickness. For the upper layer equations, (2.4.12) takes the form

$$\frac{D}{Dt^*}\left[\frac{\zeta_1^* + f}{H + s^*y^* - h^*}\right] = 0. \tag{2.4.13}$$

When we apply the scalings from Section 2.2, the equation (2.4.13) is exactly (2.4.10).

Returning to (2.4.11), if we now substitute the expansion (2.3.1), we obtain

$$PV_1 \simeq 1 + s\left(\zeta_1^{(0)} + h^{(0)} - y\right) + O\left(s^2\right). \tag{2.4.14}$$

Hence, to leading order, (2.4.10) is

$$\left(\frac{\partial}{\partial t} + u_1^{(0)}\frac{\partial}{\partial x} + v_1^{(0)}\frac{\partial}{\partial y}\right)\left(\zeta_1^{(0)} + h^{(0)} - y\right) + O(s) = 0,$$

which, if the geostrophic relations (2.3.7) are substituted in, is exactly (2.3.14).

We begin the derivation of the potential vorticity equation for the abyssal layer by taking the curl of (2.2.24), i.e.,

$$\frac{\partial}{\partial x}[\widehat{\mathbf{e}}_2 \cdot (2.2.24)] - \frac{\partial}{\partial y}[\widehat{\mathbf{e}}_1 \cdot (2.2.24)],$$

and the result is

$$u_{2x} + v_{2y} = -s\left[\frac{D\zeta_2}{Dt} + (u_{2x} + v_{2y})\zeta_2\right], \tag{2.4.15}$$

where

$$\zeta_2 = v_{2x} - u_{2y},$$

and

$$\frac{D}{Dt} = \frac{\partial}{\partial t} + u_2\frac{\partial}{\partial x} + v_2\frac{\partial}{\partial y}. \tag{2.4.16}$$

The continuity equation (2.2.25) can be written in the form

$$-\frac{1}{h}\frac{Dh}{Dt} = \nabla \cdot \mathbf{u}_2 = u_{2x} + v_{2y}, \tag{2.4.17}$$

which if it is substituted into (2.4.15) yields

$$-\frac{1}{h}\frac{Dh}{Dt} = -s\left[\frac{D\zeta_2}{Dt} - \frac{1}{h}\frac{Dh}{Dt}\zeta_2\right], \tag{2.4.18}$$

or, after multiplying by $1/h$ and rearranging, can be written as

$$\frac{s}{h}\frac{D\zeta_2}{Dt} - \frac{1 + s\zeta_2}{h^2}\frac{Dh}{Dt} = 0, \tag{2.4.19}$$

or, equivalently,

$$\frac{D}{Dt}\left(\frac{1+s\zeta_2}{h}\right)=0, \tag{2.4.20}$$

which is the potential vorticity equation for the abyssal layer. The nondimensional potential vorticity for the abyssal layer, here denoted by $PV_2$, is given by

$$PV_2=\frac{1+s\zeta_2}{h}, \tag{2.4.21}$$

and is conserved following the motion.

As was the case for the upper layer, equation (2.4.20) could also have been obtained by the scalings into the dimensional shallow water potential vorticity equation (2.4.12), as it relates to the lower layer, i.e.,

$$\frac{D}{Dt^*}\left(\frac{\zeta_2^*+f}{h^*}\right)=0. \tag{2.4.22}$$

Returning to (2.4.21), if we now substitute the expansion (2.3.1), we obtain

$$PV_2\simeq\frac{1}{h^{(0)}}+O(s). \tag{2.4.23}$$

Hence, to leading order, (2.4.20) is

$$\left(\frac{\partial}{\partial t}+u_2^{(0)}\frac{\partial}{\partial x}+v_2^{(0)}\frac{\partial}{\partial y}\right)\left(\frac{1}{h^{(0)}}\right)+O(s)=0,$$

which, if the geostrophic relations (2.3.8) are substituted in, is exactly (2.3.9).

## 2.5 Steady solutions and general stability properties

The Swaters (1991) model equations are given by, after deleting the (0)-superscript,

$$(\Delta\eta+h)_t-\eta_x+J(\eta,\ \Delta\eta+h)=0. \tag{2.5.1}$$

$$h_t + h_x + J(\eta,\ h) = 0, \tag{2.5.2}$$

with the auxiliary relations

$$\mathbf{u}_1 = \widehat{\mathbf{e}}_3 \times \nabla\eta, \tag{2.5.3}$$

$$\mathbf{u}_2 = \widehat{\mathbf{e}}_1 + \widehat{\mathbf{e}}_3 \times \nabla(\eta + h), \tag{2.5.4}$$

$$p = \eta + h - y, \tag{2.5.5}$$

where we have also deleted the 2-subscript on the abyssal layer geostrophic pressure field. From time to time it will be more convenient to work with (2.5.1) minus (2.5.2), i.e.,

$$\Delta\eta_t - \eta_x - h_x + J(\eta, \Delta\eta) = 0, \tag{2.5.6}$$

as the upper layer equation.

The boundary condition on the channel walls, given by (2.2.21), now takes the form, after substituting the geostrophic relations (2.3.7) and (2.3.8),

$$\eta_x = h_x = 0 \text{ on } y = 0, L. \tag{2.5.7}$$

The model equations (2.5.1) or (2.5.6), (2.5.2), together with the boundary conditions (2.5.7), have an exact steady nonlinear along slope solution given by

$$\left.\begin{aligned} \eta = \eta_0(y) = -\textstyle\int_0^y U_0(\xi)\,d\xi \Longrightarrow \mathbf{u}_{10} = (U_0,\ 0)\,, \\ h = h_0(y) \geq 0 \Longrightarrow \mathbf{u}_{20} = (1 - h_{0y} + U_0,\ 0)\,. \end{aligned}\right\} \tag{2.5.8}$$

for all sufficiently smooth $U_0(y)$ and $h_0(y)$. This can be verified by direct substitution. The solution (2.5.8) corresponds to a steady along slope mean flow in the upper layer with the along slope velocity given by $U_0\,(y)$ and an abyssal current height profile given by $h_0(y)$, which is invariant in the along slope direction. The abyssal along slope velocity will be given by $u_{20} = 1 - h_{0y} + U_0$.

For convenience we will henceforth assume $U_0(y) = 0$. This has the effect of removing any mean flow in the upper layer, which will eliminate any possible barotropic instability in the model. That is, we are going to explicitly focus

on the baroclinic instability of abyssal currents. We note that the effect of the barotropic instability of an upper layer flow on abyssal currents has been examined experimentally by Sutherland *et al.* (2004). Understanding the full oceanographic implications of this mechanism for the transition to instability remains an interesting problem that needs to be examined.

Linear stability analysis is a procedure in which a small perturbation is applied to a steady solution of the governing equations in order to see if such disturbances will grow with time, indicating instability, or remain constant, oscillate, or recede, indicating stability of the steady solution to such perturbations. From a physical context, we are really determining if the steady solution has the possibility of persisting in time, because it will never be seen in nature (or even in a laboratory setting) if it is susceptible to small perturbations rapidly growing since it is not possible to completely eliminate "imperfections" that give rise to small deviations from the steady solution (Drazin and Reid, 1981).

Mathematically, an analytical stability analysis is carried out by adding a small perturbation to the steady solution to be studied, and substituting this into the nonlinear governing equations. The key assumption in a linear stability analysis is that the perturbations are small, which allows us to ignore terms that are nonlinear in the perturbations (which in our context means dropping the quadratic perturbation terms). The result of applying this procedure is the so-called linear stability equations, the solution of which determines the spatial structure and temporal evolution of the disturbances.

However, it is important to point out that if there is instability in the linear stability analysis, the growing disturbance will always reach a size where the linear stability equations are no longer valid, because at that point the small perturbation assumption is violated. One then needs to appeal to nonlinear theories in order to follow the evolution in time of the disturbance, because the

nonlinear terms can no longer be ignored.

In order to derive the stability equations, we introduce

$$h = h_0(y) + h'(x, y, t), \tag{2.5.9}$$

$$\eta = \eta'(x, y, t). \tag{2.5.10}$$

where $h_0(y)$ is the steady abyssal solution (recall we have assumed $U_0(y) = 0$), and $\eta'$ and $h'$ are the perturbation quantities. We then substitute (2.5.9) and (2.5.10) into (2.5.2) and (2.5.6) to get (after dropping the primes)

$$\Delta\eta_t - \eta_x - h_x + J(\eta, \Delta\eta) = 0, \tag{2.5.11}$$

$$(\partial_t + \partial_x)\, h + h_{0y}\eta_x + J(\eta, h) = 0. \tag{2.5.12}$$

These are the *nonlinear perturbation equations*, and they will be used in the weakly nonlinear analysis presented in the next two sections.

For our purposes here, we drop the nonlinear Jacobian terms, which are quadratic in the perturbations, to arrive at the *linear stability equations*

$$\Delta\eta_t - \eta_x - h_x = 0, \tag{2.5.13}$$

$$(\partial_t + \partial_x)\, h + h_{0y}\eta_x = 0. \tag{2.5.14}$$

Before proceeding to the nonlinear stability analysis it is useful to review the known linear stability properties associated with the linear stability equations. We do this because there is certain information, essential to the weakly nonlinear work, which is generated from the linear analysis, namely the marginal stability curve, whose meaning will be discussed at length in a later section, and the dispersion relation for the perturbation modes. Our discussion here closely follows that in Swaters (1991).

The energetics associated with destabilization can be ascertained from the area-averaged perturbation energy equation for the upper layer, obtained by multiplying (2.5.13) by $\eta$ and integrating, that is,

$$\frac{\partial}{\partial t}\int_0^L\int_0^\lambda \nabla\eta\cdot\nabla\eta\; dxdy = -2\int_0^L\int_0^\lambda \eta h_x\; dxdy$$
$$= 2\int_0^L\int_0^\lambda \eta_x h\; dxdy = 2\int_0^L\int_0^\lambda v_1 h\; dxdy, \qquad (2.5.15)$$

where $\lambda$ is the wavelength of the perturbation (we are implicitly assuming that the perturbations are periodic in the along slope direction) and where it is understood that the limits of integration associated with integrals that contain $h$ in the integrand are, in fact, only over the region where $h_0 > 0$.

Thus, instability can only occur, which is equivalent to assuming

$$\frac{\partial}{\partial t}\int_0^L\int_0^\lambda \nabla\eta\cdot\nabla\eta\; dxdy > 0 \Longrightarrow \int_0^L\int_0^\lambda v_1 h\; dxdy > 0,$$

which implies that, on average over one wavelength $v_1$ is positively correlated with $h$. That is, again on average, if $h > 0$ then $v_1 > 0$, and likewise, if $h < 0$ then $v_1 < 0$. If we interpret $h > 0$ as a cold anomaly in the overlying water and $h < 0$ as a warm anomaly in the overlying water, then a positive correlation between $v_1$ and $h$ can be interpreted as a net up-slope heat transport. Since the sloping bottom is a topographic $\beta$-plane in this model, this means that instability can only occur if there is a net transport of heat up the background potential vorticity gradient. This is exactly the scenario associated with the baroclinic instability of zonal flow on a planetary $\beta$-plane (Pedlosky, 1987 and LeBlond and Mysak, 1978) and underscores the fact that the transition to instability mechanism being modelled here is a purely baroclinic one.

Additional qualitative information can be obtained by multiplying (2.5.14) by $h/h_{0y}$ and integrating, that is,

$$\frac{\partial}{\partial t}\int_0^L\int_0^\lambda \frac{h^2}{h_{0y}}\; dxdy = -2\int_0^L\int_0^\lambda v_1 h\; dxdy.$$

If this result is substituted into (2.5.15), it follows that

$$\frac{\partial}{\partial t}\left\{\int_0^L\int_0^\lambda \nabla\eta\cdot\nabla\eta + \frac{h^2}{h_{0y}}\,dxdy\right\} = 0. \tag{2.5.16}$$

Equation (2.5.16) is the perturbation energy equation and implies that the quantity in the curly brackets is an invariant of the motion, that is,

$$\int_0^L\int_0^\lambda \nabla\eta\cdot\nabla\eta + \frac{h^2}{h_{0y}}\,dxdy = \left[\int_0^L\int_0^\lambda \nabla\eta\cdot\nabla\eta + \frac{h^2}{h_{0y}}\,dxdy\right]_{t=0}. \tag{2.5.17}$$

Instability can only occur, that is the amplitude of the perturbation fields can only grow in time, if there is at least one value of $y$ in the region where $h_0 > 0$ for which $h_{0y} < 0$. Clearly, if $h_{0y} > 0$ for all values of $y$ in the region where $h_0 > 0$, then the perturbation energy is a well defined norm on the perturbation fields and the flow is linearly stable. This necessary condition for instability has been generalized to other flow profiles by Swaters (1993), to other topographic profiles by Karsten and Swaters (1996) and to other geometries by Choboter and Swaters (2000).

The fact that there must be at least one value of $y$ in the region where $h_0 > 0$ for which $h_{0y} < 0$ for instability to occur has a simple physical interpretation. If we consider an abyssal height profile which is quadratically shaped (see Fig. 1) that possesses two groundings or incroppings (the two points where $h_0$ intersects the bottom), the necessary condition for instability is only satisfied on the down slope side of the abyssal height. This serves to underscore the spatial structure of the unstable disturbances which correspond to preferentially amplifying perturbations on the down slope grounding which subsequently evolve into down slope propagating plumes (Swaters, 1991, 1998).

Further qualitative results can be obtained from the *normal mode linear instability equations* that are obtained by substituting

$$\eta = \hat{\eta}(y)\exp[ik(x-ct)] + c.c., \tag{2.5.18}$$

$$h = \hat{h}(y)\exp[ik(x - ct)] + c.c., \tag{2.5.19}$$

where $c.c.$ means the complex conjugate of the preceding term, $k$ is the real-valued along slope wavenumber, and $c$ is the along slope complex-valued wave velocity into the linear stability equations, to yield, after a little algebra

$$\hat{\eta}_{yy} - (k^2 - \frac{1}{c} - \frac{h_{0y}}{c(c-1)})\hat{\eta} = 0, \tag{2.5.20}$$

$$\hat{h} = \frac{h_{0y}}{c-1}\hat{\eta}. \tag{2.5.21}$$

The boundary conditions become

$$\hat{\eta} = \hat{h} = 0 \text{ on } y = 0, L. \tag{2.5.22}$$

Following Swaters (1991), it is possible to obtain a semi-circle theorem (Drazin and Reid, 1981) and sharp bounds on the growth rates and phase velocities for the unstable modes. If (2.5.20) is multiplied through by the complex conjugate of $\hat{\eta}$, denoted by $\hat{\eta}^*$, and the result integrated over $y$, we obtain

$$\int_0^L \left[(1 - ck^2) + \frac{(c^* - 1)\, h_{0y}}{|c-1|^2}\right] |\hat{\eta}|^2 - c\,|\hat{\eta}_y|^2 \; dy. \tag{2.5.23}$$

If we now substitute $c = c_R + ic_I$ into this balance and separate the result into the imaginary and real components, we obtain the two integrals, respectively,

$$c_I \left\{ \int_0^L |\hat{\eta}_y|^2 + \left[k^2 + \frac{h_{0y}}{|c-1|^2}\right] |\hat{\eta}|^2 \; dy \right\} = 0, \tag{2.5.24}$$

$$c_R \left\{ \int_0^L |\hat{\eta}_y|^2 + \left[k^2 - \frac{h_{0y}}{|c-1|^2}\right] |\hat{\eta}|^2 \; dy \right\}$$
$$= \int_0^L \left[1 - \frac{h_{0y}}{|c-1|^2}\right] |\hat{\eta}|^2 \; dy. \tag{2.5.25}$$

From (2.5.24) we see immediately that assuming instability occurs, i.e., $c_I > 0$, it follows that the integral inside the curly brackets must be identically zero and this can only occur, again, if there is at least one value of $y$ in the region where

$h_0 > 0$ for which $h_{0y} < 0$. Thus, assuming instability occurs, we may introduce $\gamma$, defined by

$$\min_{y \in (0,L)} h_{0y} = -\gamma < 0 \ (\Longrightarrow \gamma > 0)\,.$$

If instability occurs, then the fact that the integral inside the curly brackets in (2.5.24) must be identically zero can be re-arranged, to yield

$$|c-1|^2 = -\frac{\int_0^L h_{0y}\,|\hat{\eta}|^2\ dy}{\int_0^L\ |\hat{\eta}_y|^2 + k^2\,|\hat{\eta}|^2\ dy} \leq \gamma \frac{\int_0^L |\hat{\eta}|^2\ dy}{\int_0^L\ |\hat{\eta}_y|^2 + k^2\,|\hat{\eta}|^2\ dy} \leq \frac{\gamma}{k^2}, \qquad (2.5.26)$$

or, equivalently, that the complex valued phase speed must lie in the semicircle defined by

$$(c_R - 1)^2 + c_I^2 \leq \frac{\gamma}{k^2},\ c_I > 0. \qquad (2.5.27)$$

This, in turn, implies that, if instability occurs, that the growth rate, denoted as $\sigma$ and defined by $\sigma = kc_I$, satisfies

$$\sigma \leq \sqrt{\gamma}.$$

Additionally, if instability occurs, then we may use (2.5.26) to eliminate $|c-1|$ in (2.5.25) to yield, after a little algebra,

$$c_R = \frac{1}{2} + \frac{\int_0^L |\hat{\eta}|^2\ dy}{2\int_0^L\ |\hat{\eta}_y|^2 + k^2\,|\hat{\eta}|^2\ dy} \leq \frac{1}{2}\left(1 + \frac{1}{k^2}\right). \qquad (2.5.28)$$

Equations (2.5.27) and (2.5.28) can be used to infer the existence of a high wavenumber cutoff for instability, that is for a given $\gamma$, there exists $k_{\max}$ such that for $k > k_{\max}$ there is no instability. From (2.5.27) we see that

$$1 - \frac{\sqrt{\gamma}}{k} \leq c_R \leq 1 - \frac{\sqrt{\gamma}}{k}. \qquad (2.5.29)$$

Clearly, for sufficiently large $k$, the intervals in (2.5.29) and (2.5.28) become disjoint, i.e., their intersection is empty. Their intersection is non-empty, that is, instability can only occur if

$$1 - \frac{\sqrt{\gamma}}{k} \leq \frac{1}{2}\left(1 + \frac{1}{k^2}\right),$$

which can be re-arranged to give

$$0 \leq k \leq k_{\max} \equiv \sqrt{\gamma} + \sqrt{1+\gamma}. \tag{2.5.30}$$

Conversely, a mode with a given along slope wavenumber $k$ will be unstable only if

$$\gamma \geq \gamma_{\min} \equiv \left(\frac{k^2-1}{2k}\right)^2. \tag{2.5.31}$$

## 2.6 The abyssal flow examined in this thesis

In the remainder of this thesis we will restrict attention to the constant abyssal flow given by

$$h_0(y) = h_{\max} - \gamma y, \tag{2.6.1}$$

where we assume $h_{\max} - \gamma y > 0$ for $y \in (0, L)$. Here $\gamma$ is the cross slope rate of change of the thickness of the abyssal current height relative to the sloping bottom. The dimensional rate of change is given by $\gamma^* = (h^*/L^*)\gamma$. Clearly, the height profile given by (2.6.1) will satisfy the necessary conditions for instability. We use the same profile which is used by Mooney and Swaters (1996).

Here we review the linear instability theory for the constant abyssal flow given by (2.6.1). If (2.6.1) is substituted into the normal mode equations (2.5.20) and (2.5.21), one obtains

$$\hat{\eta}_{yy} - (k^2 - \frac{1}{c} + \frac{\gamma}{c(c-1)})\hat{\eta} = 0, \tag{2.6.2}$$

$$\hat{h} = -\frac{\gamma}{c-1}\hat{\eta}, \tag{2.6.3}$$

with the boundary conditions

$$\hat{\eta} = \hat{h} = 0 \quad \text{on } y = 0,\ L. \tag{2.6.4}$$

The solution to (2.6.2) subject to (2.6.4) is

$$\hat{\eta} = a_1 \sin(n\pi y/L). \tag{2.6.5}$$

where $a_1$ is a free constant and $n = 1, 2, 3, \ldots$ . Therefore, the general form of the normal mode solution is given by

$$\eta = a_1 \sin(ly) \exp[ik(x - ct)] + c.c., \tag{2.6.6}$$

$$h = -a_1 \frac{\gamma}{c-1} \sin(ly) \exp[ik(x - ct)] + c.c., \tag{2.6.7}$$

where $l = n\pi/L$.

When we substitute (2.6.6) into (2.6.2), we get an expression for $c$, which is

$$c = \frac{k^2 + l^2 + 1 \pm [(k^2 + l^2 + 1)^2 - 4(k^2 + l^2)(1 + \gamma)]^{1/2}}{2(k^2 + l^2)}. \tag{2.6.8}$$

Equation (2.6.8) is a formula that expresses $c$ as a function of $k$ and $l$. This is called a *dispersion relation* because it shows that waves of different wavelengths travel at different phase speeds, that is, they disperse (Kundu, 1990).

For instability to occur, the imaginary part of $c$ must be positive. The boundary between instability and stability will be given, therefore, when the quantity inside the square root term in (2.6.8) is zero. This gives us the marginal stability curve, with the critical value $\gamma_c$ of $\gamma$,

$$\gamma_c = (K^2 - 1)^2/4K^2, \tag{2.6.9}$$

where $K$ is the total wavenumber, given by,

$$K^2 = k^2 + l^2, \tag{2.6.10}$$

that is a mode with total wavenumber $K$ is unstable if and only if $\gamma > \gamma_c$. Alternatively, the marginal stability curve represents the boundary between stable modes and unstable modes for a particular $\gamma_c$.

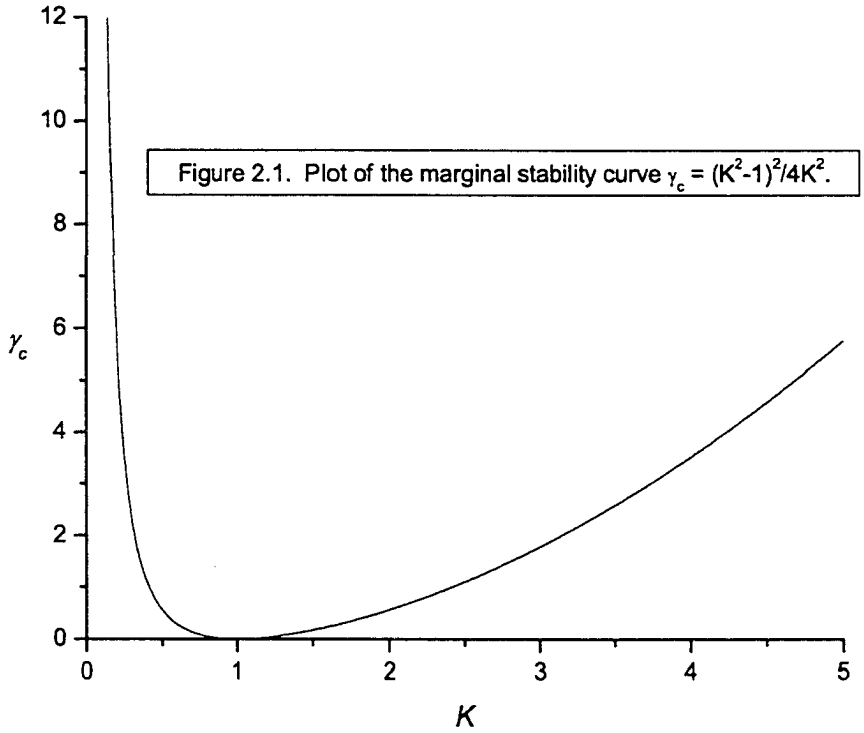


In Fig. 2.1 we present the marginal stability curve as determined by (2.6.9). The minimum of the marginal stability curve is located at $K = 1$ and corresponds to $\gamma_c = 0$. The *point of marginal stability* corresponds to the first value of $\gamma$ for which any larger value of $\gamma$ leads to instability. The point of marginal instability therefore corresponds to $\gamma_c = 0$ and $K = 1$. Clearly, the $K = 1$ mode can only exist if $l \leq 1$ for some value of $n$. Consequently, we shall henceforth assume that $n = 1$ so that $l = \pi/L$ (the gravest, or first, cross slope mode).

# Chapter 3

# Weakly nonlinear evolution of $K \neq 1$ unstable modes

In order to see how the marginally unstable modes as determined by linear theory actually evolve in time we must allow the nonlinear interactions to be included in the description. That is, we must develop a finite amplitude instability theory which follows the evolution of the wave when it has reached amplitudes for which the linear theory is no longer valid.

In this section, we derive a temporal amplitude evolution equation for a weakly sub or supercritical mode which has a wavenumber modulus *different* than $K = 1$. It is important to realize that in this situation, there will always be other modes with different wavenumbers which are unstable at smaller values of $\gamma$. Because of this, in this section we do not introduce a slow space variable which would follow the evolution of a wave packet centered on the mode in question. It is straightforward to include a slow space variable for these modes in a similar manner as that described, for example, for the Phillips' model for baroclinic

instability of a zonal flow on a $\beta$-plane (Tan and Liu, 1995).

Also, we point out that in some sense the analysis presented in this section is somewhat artificial in that there will always be wavenumber moduli $K$ for the same $\gamma$ that are more unstable than the wavenumber being considered. Nevertheless, it is instructive, if not the most physically relevant, to consider a marginally sub or supercritical $K \neq 1$ mode. We remark that the theory developed in this section is, in fact, the nonlinear generalization of the theory developed by Pavec *et al.* (2004), which is itself based on the work of Pedlosky and Thomson (2003). Or, from another point of view, this section extends the nonlinear instability theory described in Section 4 in Mooney and Swaters (1996) to the case where the marginally sub or supercritical abyssal current varies slowly with respect to time.

## 3.1 Developing the asymptotic expansion

We have to develop a finite amplitude theory that follows the evolution of the marginally unstable wave when it has reached amplitudes for which the linear theory is no longer valid. Weakly nonlinear analysis can be used to derive the nonlinear amplitude equation if the mode is weakly unstable. In this section, we use weakly nonlinear analysis to derive an amplitude evolution equation which follows the evolution of the disturbance associated with a slightly supercritical mode when the height, and thus the velocity, of the abyssal current has time variability, but on a slower time scale than the fast phase period of the underlying mode.

To determine the proper scaling for the slow time variable we examine the dispersion relation (2.6.8) in the situation when $\gamma$ is slightly supercritical. If, for the moment, we assume that

$$\gamma = \gamma_c + \delta,$$

where $\delta$ is a small positive number (i.e., the supercriticality), the dispersion relation (2.6.8) becomes

$$c = \frac{K^2 + 1 \pm [(K^2+1)^2 - 4K^2(1+\gamma_c+\delta)]^{1/2}}{2K^2},$$

where we recall that $K = \sqrt{k^2+l^2} > 0$. Substituting in for $\gamma_c$ from (2.6.9) gives

$$\begin{aligned} c &= \frac{K^2 + 1 \pm [(K^2+1)^2 - 4K^2(1+\frac{(K^2-1)^2}{4K^2}+\delta)]^{1/2}}{2K^2} \\ &= \frac{K^2 + 1 \pm \{-4K^2\delta\}^{\frac{1}{2}}}{2K^2} = \frac{K^2+1}{2K^2} \pm i\frac{\sqrt{\delta}}{K}. \end{aligned} \tag{3.1.1}$$

Examining (3.1.1), we see that the linear growth rate, given by $\sigma = kc_I$, where $c_I$ is the (positive) imaginary part of $c$, is given by

$$\sigma = \frac{k\sqrt{\delta}}{K}. \tag{3.1.2}$$

Thus, the linear growth rate will be proportional to $\sqrt{\delta}$ so that the $e$-folding time scale associated with the slightly supercritical mode will be $O\left(1/\sqrt{\delta}\right)$. The assumptions for the asymptotic expansion must be such that the time scale over which the nonlinear interactions make a cumulative $O(1)$ contribution to the evolution of the marginally unstable mode is the same as the linear growth rate.

Following and extending the ideas of Mooney and Swaters (1996) and Pedlosky and Thomson (2003) to allow for time variations in the slightly sub or supercritical abyssal current, we will choose $\delta$ to be of the form

$$\delta = \varepsilon^2 \left[\Upsilon_0 + \Upsilon(\varepsilon t)\right],$$

where $\Upsilon_0 = \pm 1$ ($\Upsilon_0 = +1$ and $\Upsilon_0 = -1$ correspond to a slightly supercritical or subcritical abyssal current, respectively), and $\Upsilon(\varepsilon t)$ is an $O(1)$ real-valued function of time that models the temporal variations of the marginally stable or unstable abyssal flow. We will choose a specific form for $\Upsilon(\varepsilon t)$ when we describe

the solutions to the yet-to-be derived nonlinear amplitude equation. The parameter $\varepsilon$ is assumed to satisfy $0 < \varepsilon << 1$ and corresponds to the nondimensional order of magnitude of the amplitude of the perturbation. We note that with this form of $\delta$, it follows that the underlying abyssal current we are examining the stability of is given by

$$h_0 = h_{\max} - \left\{\gamma_c + \varepsilon^2 \left[\Upsilon_0 + \Upsilon\left(\varepsilon t\right)\right]\right\} y$$

$$\Longrightarrow \mathbf{u}_{20} = \left(1 + \gamma_c + \varepsilon^2 \left[\Upsilon_0 + \Upsilon\left(\varepsilon t\right)\right]\right) \widehat{\mathbf{e}}_1.$$

There are, of course, many possible choices that one could make for $\delta$. But the reason to choose this specific form is that this choice will allow the time scale of the growth of the amplitude of the perturbations to balance the time scale associated with the nonlinear interactions and the time variations of the abyssal current. In summary, with this choice of $\delta$, $\gamma$ is given by

$$\gamma = \gamma_c + \varepsilon^2 \left[\Upsilon_0 + \Upsilon\left(\varepsilon t\right)\right], \tag{3.1.3}$$

where $\gamma_c = \gamma_c\left(K\right)$ as given by (2.6.9) where it is explicitly assumed that $K \neq 1$.

Under these assumptions, we introduce the weakly nonlinear and slow time scalings

$$\eta(x, y, t) = \varepsilon \tilde{\eta}(x, y, t, T; \varepsilon), \tag{3.1.4}$$

$$h(x, y, t) = \varepsilon \tilde{h}(x, y, t, T; \varepsilon), \tag{3.1.5}$$

$$T = \varepsilon t, \tag{3.1.6}$$

where $\tilde{\eta}$ and $\tilde{h}$ are both assumed to be $O\left(1\right)$. We note that

$$T \approx O(1) \iff t \approx O(\varepsilon^{-1}), \tag{3.1.7}$$

is the time scale over which the mode will evolve nonlinearly. In addition, we observe that time derivatives will map according to $\partial_t \rightarrow \partial_t + \varepsilon \partial_T$.

If (2.6.1), (3.1.3), (3.1.4), (3.1.5) and (3.1.6) are substituted into the nonlinear perturbation equations (2.5.11) and (2.5.12), and the tildes dropped, we obtain

$$\varepsilon\left(\partial_t + \varepsilon\partial_T\right)\Delta\eta - \varepsilon\eta_x - \varepsilon h_x + \varepsilon^2 J(\eta,\ \Delta\eta) = 0, \tag{3.1.8}$$

$$\varepsilon\left(\partial_t + \varepsilon\partial_T + \partial_x\right)h - \varepsilon\left\{\gamma_c + \varepsilon^2\left[\Upsilon_0 + \Upsilon\left(\varepsilon t\right)\right]\right\}\eta_x + \varepsilon^2 J(\eta,\ h) = 0, \tag{3.1.9}$$

which can be re-arranged into the form

$$\Delta\eta_t - \eta_x - h_x = -\varepsilon\Delta\eta_T - \varepsilon J(\eta, \Delta\eta), \tag{3.1.10}$$

$$h_t + h_x - \gamma_c\eta_x = -\varepsilon h_T + \varepsilon^2\left[\Upsilon_0 + \Upsilon\left(T\right)\right]\eta_x - \varepsilon J(\eta, h). \tag{3.1.11}$$

We follow the method in Mooney and Swaters (1996), and solve (3.1.10) and (3.1.11) with an expansion of the form

$$\eta(x, y, t, T; \varepsilon) = \eta_0(x, y, t, T) + \varepsilon\eta_1(x, y, t, T) + \varepsilon^2\eta_2(x, y, t, T) + \cdots\ , \tag{3.1.12}$$

$$h(x, y, t, T; \varepsilon) = h_0(x, y, t, T) + \varepsilon h_1(x, y, t, T) + \varepsilon^2 h_2(x, y, t, T) + \cdots\ . \tag{3.1.13}$$

## 3.2 The $O\left(1\right)$ problem

The $O(1)$ equations are given by

$$\Delta\eta_{0t} - \eta_{0x} - h_{0x} = 0, \tag{3.2.1}$$

$$h_{0t} + h_{0x} - \gamma_c\eta_{0x} = 0, \tag{3.2.2}$$

and are simply the linear stability equations (2.5.13) and (2.5.14). The normal mode solution for the $O(1)$ problem can be written in the form

$$\eta_0(x, y, t, T) = A(T)\sin(ly)\exp\left[ik(x - ct)\right] + c.c., \tag{3.2.3}$$

$$h_0(x, y, t, T) = B(T)\sin(ly)\exp\left[ik(x - ct)\right] + c.c.\ . \tag{3.2.4}$$

Substituting (3.2.3) and (3.2.4) into (3.2.1) and (3.2.2) gives the pair of algebraic equations

$$\begin{bmatrix} K^2c-1 & -1 \\ -\gamma_c & -c+1 \end{bmatrix} \begin{pmatrix} A \\ B \end{pmatrix} = 0. \tag{3.2.5}$$

Since we are only interested in nontrivial solutions it follows that the determinant of the coefficient matrix in (3.2.5) must be identically zero, i.e.,

$$\left(K^2c-1\right)(1-c) = \gamma_c.$$

If (2.6.9) is substituted into this expression, it follows (as it must, see (3.1.2)), that

$$c = \frac{K^2+1}{2K^2}. \tag{3.2.6}$$

If (3.2.6) is substituted into (3.2.5), it also follows that

$$B = \frac{\gamma_c}{1-c}A = \frac{1}{2}(K^2-1)A, \tag{3.2.7}$$

which determines the amplitude of the perturbation height of the abyssal current as a function of the normal mode amplitude in the overlying water column.

Hence, we have determined the spatial and fast time structure of the $O(1)$ solutions. But the slow time evolution of the amplitude coefficient $A(T)$ remains undetermined. Its determination requires that we fully solve the $O(\varepsilon)$ problem and, as it turns out, examine in some detail the $O(\varepsilon^2)$ problem. This we now do.

## 3.3 The $O(\varepsilon)$ problem

The $O(\varepsilon)$ equations are given by

$$\Delta\eta_{1t} - \eta_{1x} - h_{1x} = -\Delta\eta_{0T} - J(\eta_0, \Delta\eta_0), \tag{3.3.1}$$

$$h_{1t} + h_{1x} - \gamma_c\eta_{1x} = -h_{0T} - J(\eta_0, h_0). \tag{3.3.2}$$

The first thing to note is that if (3.2.3) and (3.2.4) are substituted into the right-hand-side (R.H.S) of (3.3.1) and (3.3.2), the Jacobian terms are identically zero, so that (3.3.1) and (3.3.2) reduce to

$$\Delta\eta_{1t} - \eta_{1x} - h_{1x} = A_T K^2 \sin(ly) \exp[ik(x - ct)] + c.c., \tag{3.3.3}$$

$$h_{1t} + h_{1x} - \gamma_c \eta_{1x} = -\frac{\gamma_c}{1-c} A_T \sin(ly) \exp[ik(x - ct)] + c.c.\ . \tag{3.3.4}$$

The solution for (3.3.3) and (3.3.4) may be written in the general form

$$\eta_1 = E(T) \sin(ly) \exp[ik(x - ct)] + c.c., \tag{3.3.5}$$

$$h_1 = \phi(y, T) + F(T) \sin(ly) \exp[ik(x - ct)] + c.c., \tag{3.3.6}$$

where $\phi(y, T)$ is a real-valued homogeneous solution which will be required to balance adjustments to the mean flow resulting from nonlinear interactions that arise in the $O(\varepsilon^2)$ problem. Substituting (3.3.5) and (3.3.6) into (3.3.4) implies that

$$F - \frac{\gamma_c}{1-c} E = \frac{i\gamma_c}{k(1-c)^2} A_T,$$

and hence

$$F = \frac{\gamma_c E}{1-c} + \frac{i\gamma_c A_T}{k(1-c)^2}. \tag{3.3.7}$$

Further, if (3.3.5) and (3.3.6) are substituted into (3.3.3), with $F$ given by (3.3.7), it follows, after a little algebra, that

$$E\left(c - \frac{K^2 + 1}{2K^2}\right) = E \cdot 0 = 0, \tag{3.3.8}$$

where we have used (2.6.9) and (3.2.6).

Two important facts follow from (3.3.8). First, there are no inhomogeneities in (3.3.8). Thus, the inhomogeneities in (3.3.3) and (3.3.4) do not provide any constraint on the evolution of the leading order amplitude $A(T)$. Second, (3.3.8) is satisfied for all $E(T)$. This implies that the "$E$ mode" in (3.3.5) is not required to contribute to a particular solution for the $O(\varepsilon)$ problem. That is, the

"$E$ mode" corresponds to a homogenous solution and is thus just an additional contribution to the $O(1)$ solution. We may thus "absorb" this contribution directly into the $O(1)$ solution (Pedlosky, 1970) and, without loss of generality, set $E = 0$. Consequently, the $O(\varepsilon)$ solution can be written in the form

$$\eta_1(x, y, t, T) = 0, \tag{3.3.9}$$

$$h_1(x, y, t, T) = \phi(y, T) + \left\{ \frac{i\gamma_c A_T}{k(1-c)^2} \sin(ly) \exp\left[ik(x - ct)\right] + c.c. \right\}. \tag{3.3.10}$$

The $O(\varepsilon)$ problem has not determined the evolution of $A(T)$ and has, in fact, introduced a new undetermined function $\phi(y, T)$. Both of these functions will be determined by examining the $O(\varepsilon^2)$ problem.

## 3.4 The $O\left(\varepsilon^2\right)$ problem

The $O(\varepsilon^2)$ equations are given by

$$\Delta\eta_{2t} - \eta_{2x} - h_{2x} = -\Delta\eta_{1T} - \eta_{0x}\Delta\eta_{1y} - \eta_{1x}\Delta\eta_{0y} + \eta_{0y}\Delta\eta_{1y} + \eta_{1y}\Delta\eta_{0x}, \tag{3.4.1}$$

$$h_{2t} + h_{2x} - \gamma_c\eta_{2x} = -h_{1T} + \left[\Upsilon_0 + \Upsilon(T)\right]\eta_{0x} - J(\eta_1, h_0) - J(\eta_0, h_1), \tag{3.4.2}$$

which reduce, since $\eta_1(x, y, t, T) = 0$, to

$$\Delta\eta_{2t} - \eta_{2x} - h_{2x} = 0, \tag{3.4.3}$$

$$h_{2t} + h_{2x} - \gamma_c\eta_{2x} = -h_{1T} + \left[\Upsilon_0 + \Upsilon(T)\right]\eta_{0x} - J(\eta_0, h_1), \tag{3.4.4}$$

which further reduce, if $\eta_0(x, y, t, T)$ and $h_1(x, y, t, T)$ are substituted into the right-hand-sides, to

$$\Delta\eta_{2t} - \eta_{2x} - h_{2x} = 0, \tag{3.4.5}$$

$$h_{2t} + h_{2x} - \gamma_c\eta_{2x} =$$

$$\left\{ -\frac{i\gamma_c A_{TT}}{k(1-c)^2} + Aik\left[\Upsilon_0 + \Upsilon(T) - \phi_y\right] \right\} \sin(ly) \exp(ik\theta) + c.c.$$

$$- \phi_T - 2l \sin(ly) \cos(ly) \gamma_c (|A|^2)_T / (1-c)^2, \tag{3.4.6}$$

where, for convenience, we have introduced $\theta = x - ct$.

Now we apply appropriate solvability conditions to (3.4.5) and (3.4.6) in order to determine the amplitude equation. First, we observe that each term in the left-hand-side of (3.4.6) contains derivatives in either $x$ or $t$. There are no terms without these derivatives. However, we notice that term

$$\phi_T + 2l \sin(ly) \cos(ly) \frac{\gamma_c (|A|^2)_T}{(1-c)^2},$$

in the right-hand-side of (3.4.6) does not contain any dependence on either $x$ or $t$. Unless this term is zero, the particular solution associated with this term, in an initial value problem where the contribution associated with this term is initially zero, will necessarily grow linearly with respect to $t$. But if this is the case, then the asymptotic expansion will no longer be asymptotically valid for $t \simeq O(\varepsilon^{-1})$. From a physical interpretation, solutions which grow linearly in time imply that there exists the possibility of an infinite amount of energy associated with the perturbations. This is not an acceptable physical result. Thus we are forced to conclude that

$$\phi_T + 2l \sin(ly) \cos(ly) \frac{\gamma_c (|A|^2)_T}{(1-c)^2} = 0,$$

which implies that

$$\phi(y, T) = -l \sin(2ly) \frac{\gamma_c (|A|^2 - |A_0|^2)}{(1-c)^2},$$

where $A_0 = A(T = 0)$.

Further analysis is facilitated by eliminating $h_2$ from the $O(\varepsilon^2)$ equations. We begin by writing (3.4.5) and (3.4.6) in the form

$$h_{2x} = \Delta \eta_{2t} - \eta_{2x}, \tag{3.4.7}$$

$$h_{2t} + \Delta \eta_{2t} - \eta_{2x} - \gamma_c \eta_{2x} =$$

$$\left\{-\frac{i\gamma_c A_{TT}}{k(1-c)^2}+Aik\left[\Upsilon_0+\Upsilon\left(T\right)-\phi_y\right]\right\}\sin(ly)\exp(ik\theta)+c.c., \tag{3.4.8}$$

where it is understood that

$$\phi_y=-2l^2\cos(2ly)\frac{\gamma_c(|A|^2-|A_0|^2)}{(1-c)^2}.$$

If we differentiate (3.4.8) with respect to $x$, we obtain

$$h_{2tx}+\Delta\eta_{2tx}-\eta_{2xx}-\gamma_c\eta_{2xx}=$$

$$\left\{\frac{\gamma_c A_{TT}}{(1-c)^2}-Ak^2\left[\Upsilon_0+\Upsilon\left(T\right)-\phi_y\right]\right\}\sin(ly)\exp(ik\theta)+c.c., \tag{3.4.9}$$

and from (3.4.7) it follows that

$$h_{2xt}=\Delta\eta_{2tt}-\eta_{2xt}. \tag{3.4.10}$$

Substituting (3.4.10) into (3.4.9) gives us

$$(\partial_t+\partial_x)(\Delta\partial_t-\partial_x)\eta_2-\gamma_c\eta_{2xx}=$$

$$\left[\frac{\gamma_c A_{TT}}{(1-c)^2}-k^2\left[\Upsilon_0+\Upsilon\left(T\right)\right]A-\frac{2\gamma_c k^2l^2A}{(1-c)^2}(|A|^2-|A_0|^2)\cos(2ly)\right]$$
$$\times\exp(ik\theta)\sin(ly)+c.c. \tag{3.4.11}$$

And if we use the trigonometric identity

$$\cos(2ly)\sin(ly)=\frac{\sin(3ly)-\sin(ly)}{2}, \tag{3.4.12}$$

the right-hand-side of (3.4.11) becomes

$$\left[\frac{\gamma_c A_{TT}}{(1-c)^2}-k^2\left[\Upsilon_0+\Upsilon\left(T\right)\right]A+\frac{\gamma_c k^2l^2A}{(1-c)^2}(|A|^2-|A_0|^2)\right]\sin(ly)\exp(ik\theta)$$

$$-\frac{\gamma_c k^2l^2A}{(1-c)^2}(|A|^2-|A_0|^2)\sin(3ly)\exp(ik\theta)+c.c.\ . \tag{3.4.13}$$

The only terms which will produce secular growth are those terms on the right hand side of (3.4.13) that are proportional to $\sin(ly)\exp(ik\theta)$. Thus to remove the

possibility of secular growth, we set those terms on the right hand side of (3.4.13) that are proportional to $\sin(ly)\exp(ik\theta)$ to be zero, which yields the amplitude equation

$$\begin{aligned} A_{TT} &= \frac{k^2}{K^2}\left[\Upsilon_0 + \Upsilon(T)\right]A - k^2 l^2 A(|A|^2 - |A_0|^2) \\ &= \sigma^2\left[\Upsilon_0 + \Upsilon(T)\right]A - NA(|A|^2 - |A_0|^2), \end{aligned} \tag{3.4.14}$$

where

$$\sigma^2 = \frac{k^2}{K^2} > 0, \; N = k^2 l^2 > 0. \tag{3.4.15}$$

Note that $\sigma = k/K > 0$ in equation (3.4.14) is the linear growth rate for the slightly unstable mode when $\Upsilon_0 = +1$ and will be the frequency for the marginally stable mode when $\Upsilon_0 = -1$. This is in precise agreement with the linear theory as seen in (3.1.2). Assuming $\Upsilon_0 = +1$ and $\Upsilon = 0$ and neglecting the nonlinear term in (3.4.14) we can easily see the linear solution $A(T) = A_0\exp(\sigma T)$ (assuming $A(0) = A_0$ and $A_T(0) = \sigma A_0$). However, in the nonlinear problem as $A$ "grows" from the initial value $A_0$, the nonlinear term $NA(|A|^2 - |A_0|^2)$ becomes larger. Since the coefficient of the nonlinear term is negative, we see that it is possible that the nonlinear term can act to halt the "initial" exponential growth and either allow a new equilibrium amplitude to emerge or set up a nonlinear oscillation in $A(T)$. Mooney and Swaters (1996) were able to explicitly solve (3.4.14) when $\Upsilon = 0$. We are interested in examining how the solutions found by Mooney and Swaters (1996) change when the periodic forcing term in (3.4.14) is retained.

## 3.5 Solving the amplitude equation

The method of solution for (3.4.14) follows Pedlosky (Chapter 7, 1987) or as described by Mooney and Swaters (1996). We write $A(T)$ in the form

$$A(T) = R(T)\exp\left[i\theta(T)\right], \tag{3.5.1}$$

where $R(T)$ and $\theta(T)$ are real valued functions. Substituting into (3.5.1) into (3.4.14), we get

$$R_{TT} + 2iR_T\theta_T + iR\theta_{TT} - R\theta_T^2 = \sigma^2 \left[\Upsilon_0 + \Upsilon\left(T\right)\right] R - NR(R^2 - R_0^2), \quad (3.5.2)$$

where $R_0 = A_0$.

After separating the real and imaginary parts of equation (3.5.2), we get, respectively,

$$R_{TT} + R\theta_T^2 = \sigma^2 \left[\Upsilon_0 + \Upsilon\left(T\right)\right] R - NR(R^2 - R_0^2). \quad (3.5.3)$$

$$R\theta_{TT} + 2R_T\theta_T = 0. \quad (3.5.4)$$

It follows from (3.5.4), that

$$\frac{d}{dT}\left(R^2\theta_T\right) = 0,$$

which can be immediately integrated to yield

$$\theta_T = \frac{\theta_T\left(0\right) R_0^2}{R^2}.$$

We are interested in the case where $A\left(0\right) = A_0$ and $A_T\left(0\right) = \sigma A_0$ (i.e., the marginally unstable mode is initially amplifying at the linear marginal growth rate when $\Upsilon_0 = +1$). Since, in general,

$$A(0) = R(0)\exp\left[i\theta(0)\right],$$

$$A_T\left(0\right) = \left\{R_T(0) + i\theta_T\left(0\right) R(0)\right\}\exp\left[i\theta(0)\right],$$

this will be realized if

$$R(0) = A_0,\ R_T(0) = \sigma A_0,\ \theta(0) = 0,\ \theta_T\left(0\right) = 0.$$

It follows that $\theta(T) = 0$ for all $T \geq 0$.

Thus, (3.5.2) reduces to

$$R_{TT} = \sigma^2 \left[\Upsilon_0 + \Upsilon\left(T\right)\right] R - NR(R^2 - R_0^2), \quad (3.5.5)$$

subject to

$$R(0) = R_0,\ R_T(0) = \sigma R_0. \tag{3.5.6}$$

There are two cases that need to be examined. First, we describe the role that periodic time variability can play for a marginally *unstable* mode, i.e., $\Upsilon_0 = +1$. Second, we will examine the role that periodic time variability plays for a marginally *stable* mode, i.e., $\Upsilon_0 = -1$.

### The solution for $R(T)$ when $\Upsilon_0 = 1$ and $\Upsilon(T) = 0$

Since we wish to compare the role of $\Upsilon(T)$ in modifying the Mooney and Swaters (1996) solution for $R(T)$, it is appropriate to review the solution to (3.5.5) in the limit $\Upsilon_0 = 1$ and $\Upsilon(T) = 0$. If we assume that $\Upsilon_0 = 1$ and $\Upsilon(T) = 0$, (3.5.5) reduces to

$$R_{TT} = \sigma^2 R - NR(R^2 - R_0^2). \tag{3.5.7}$$

If (3.5.7) is multiplied by $R_T$ and integrated, we obtain

$$\frac{1}{2}{R_T}^2 + V(R) = \left[\frac{1}{2}{R_T}^2 + V(R)\right]_{T=0} = \frac{(\sigma R_0)^2}{2} + V(R_0), \tag{3.5.8}$$

where

$$V(R) = -\frac{R^2}{2}[\sigma^2 + N{R_0}^2] + \frac{NR^4}{4}.$$

We may re-write (3.5.8) in the form

$$d\tau = \frac{d\xi}{[(1-\xi^2)(\xi^2 - \alpha^2)]^{\frac{1}{2}}}, \tag{3.5.9}$$

where

$$\xi \equiv \frac{R}{R_{\max}},\ \alpha \equiv \frac{R_{\min}}{R_{\max}},\ \text{and}\ \tau \equiv \sqrt{(NR_{\max}^2/2)}T,$$

and where

$$R^2_{\max,\min} \equiv {R_0}^2 + \frac{\sigma^2}{N}\left[1 \pm \left(1 + \frac{2N{R_0}^2}{\sigma^2}\right)^{\frac{1}{2}}\right], \tag{3.5.10}$$

where the "max" and "min" are associated with the plus and minus signs, respectively.

Integrating (3.5.9) leads to

$$\xi = dn(\tau - \tau_0|m), \tag{3.5.11}$$

where

$$\tau_0 = dn^{-1}\left(\frac{R_0}{R_{\max}} \mid m\right). \tag{3.5.12}$$

Here $dn$ is the Jacobi elliptic dnoidal function, $m \equiv 1 - \alpha^2$, and $\tau_0$ is chosen to ensure that $R = R_0$ at $\tau = 0$.

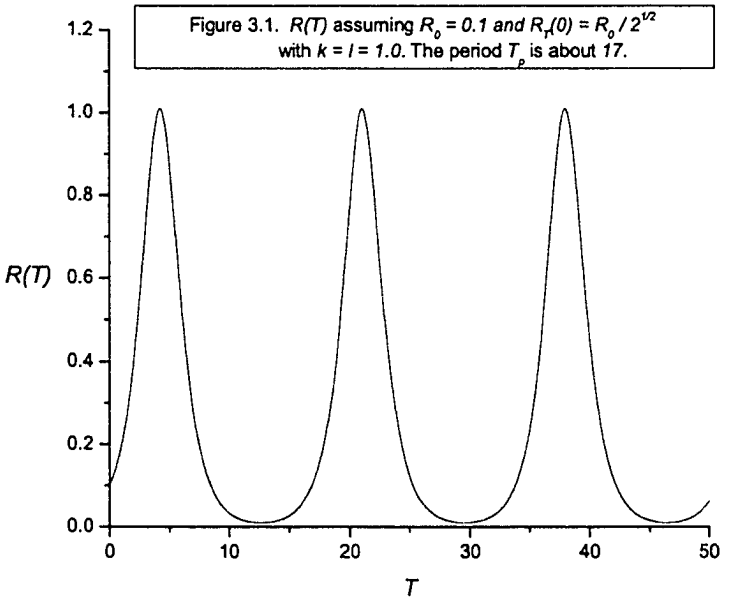


The period of the disturbance, with respect to the variable $\tau$, denoted as $\tau_p$, is given by

$$\tau_p = 2E(m),$$

where $E(m)$ is the complete Jacobi elliptic integral of the first kind. Hence, the period of the disturbance , with respect to the variable $T$, denoted as $T_p$, will be given by

$$T_p = \sqrt{8/\left(NR_{\max}^2\right)}E(m). \tag{3.5.13}$$

The evolution of $R(T)$ (and hence $A(T)$) follows the form of a dnoidal wave, and therefore is periodic in time. This means that after the initial exponential increase of the unstable mode, the effect of the nonlinearities in the equations for $A$ is to slow and eventually reverse the growth of the disturbance. The amplitude falls until it reaches a point where the linear growth rate becomes dominant again, and the cycle begins anew. In Fig. 3.1 we show a graph of the amplitude function $R(T)$ *vs.* $T$ for the parameter values given by $k = l = 1.0$ and $R_0 = 0.1$. It follows that $K = \sqrt{2}$, $\sigma = 1/\sqrt{2}$, $N = 1.0$, $R_{\max} \simeq 1.09902$, $R_{\min} \simeq 0.009902$ and $T_p \simeq 17.003033$.

**The evolution of $R(T)$ when $\Upsilon_0 = 1$ and $\Upsilon(T) \neq 0$**

In order to describe the effect of a nonzero $\Upsilon(T)$ on the Mooney and Swaters solution for $R(T)$ it is useful to select a particular form for $\Upsilon(T)$. To be consistent with Pavec *et al.* (2004) and Thomson and Pedlosky (2003) and, more importantly, for genuine oceanographic reasons, we choose the periodic function

$$\Upsilon(T) = \mathcal{H}\sin(\omega T), \tag{3.5.14}$$

where $\mathcal{H} > 0$ is the maximum amplitude and $\omega$ is the frequency of the time variation. Since $\Upsilon(0) = 0$, there will be brief period of time near $T = 0$ where we can expect the effect of $\Upsilon(T)$ to be minimal. The period of $\Upsilon(T)$, denoted by $P_\omega$, is given by $P_\omega = 2\pi/\omega$. Substitution of (3.5.14) into (3.5.5) leads to

$$R_{TT} = \sigma^2\left[1 + \mathcal{H}\sin(\omega T)\right]R - NR(R^2 - R_0^2).$$

This is a nonlinear *Mathieu Equation* (Morse and Feshbach, 1953).

In the linear limit ($N = 0$), this equation reduces to the linear Mathieu equation

$$R_{TT} - \sigma^2 \left[1 + \mathcal{H} \sin(\omega T)\right] R = 0.$$

This equation has interesting stability properties (see, for example, Sec. 11.4 in Bender and Orszag, 1978). Note that if $\mathcal{H} = 0$, then the solution to the linearized equation, subject to the initial conditions (3.5.6), is simply $R(T) = R_0 \exp(\sigma T)$, reflecting the exponential growth of the marginally unstable normal mode. However, in the above linearized Mathieu equation, it is known (see, for example, Sec. 11.4 in Bender and Orszag, 1978) that there exists a "small" region of parameter values in $(\sigma^2/\omega^2,\ \mathcal{H})$-space for which *all* solutions are stable. Hence, even in the linear limit, periodic time variability can stabilize, what is in the time averaged sense, an unstable abyssal flow.

However, as we have mentioned above, the set of $(\sigma^2/\omega^2,\ \mathcal{H})$ values for which this stabilization can occur corresponds to a very small region in parameter space. The generic solution, for most parameter values, to the above linearized Mathieu equation remains unstable, i.e., amplifying in time. Thus, the remainder of our discussion in this subsection will be focussed on describing the effect of time variability in the situation where instability persists even in the linear limit.

Specifically, we are interested in describing the effect of $\Upsilon(T)$ on the Mooney and Swaters solutions when the magnitude of $\mathcal{H}$ is small compared to the steady part of the supercriticality (i.e., $0 < \mathcal{H} << 1$), when the magnitude of $\mathcal{H}$ is comparable to the steady part of the supercriticality (i.e., $\mathcal{H} = 1$), and when the magnitude of $\mathcal{H}$ is large compared to the steady part of the supercriticality (i.e., $\mathcal{H} >> 1$). To this end, we examine the set of $\mathcal{H}$ values given by

$$\mathcal{H} \in (0.1,\ 1.0,\ 10.0). \tag{3.5.15}$$

For this set of $\mathcal{H}$ values (i.e., 0.1, 1.0 and 10.0), the abyssal flow remains slightly

unstable, has isolated single moments of marginal stability, and alternating periodic intervals of stability and instability, respectively.

With respect to the period of $\Upsilon(T)$, we are interested in examining the effect of the time variability when $P_\omega$ is short, comparable and long compared to $T_p$. To this end, we examine the set of $P_\omega$ values given by

$$P_\omega \in (10T_p,\ T_p,\ T_p/10)\,, \tag{3.5.16}$$

which implies that we will examine the set of frequencies given by

$$\omega \in (\pi/(5T_p)\,,\ 2\pi/T_p,\ 20\pi/T_p)\,. \tag{3.5.17}$$

In summary, we will describe the set of nine simulations, labelled $S_1, S_2, \cdots, S_9$, respectively, for the $\omega$ and $\mathcal{H}$ parameters values given in Table 1. All other parameter values in this set of simulations will be identical to those associated with Fig. 3.1, i.e., $k = l = 1.0$ and $R_0 = 0.1$. It follows that $K = \sqrt{2}$, $\sigma = 1/\sqrt{2}$, $N = 1.0$, and the initial conditions are given by $R(0) = R_0$ and $R_T(0) = \sigma R_0$. The solutions for $R(T)$ were all obtained numerically by using the routine *NDSolve* in the symbolic software package *Mathematica 4.0*. Each simulation was of sufficient length in "time," i.e., with respect to $T$, so that the temporal behavior of $R(T)$ could be discerned.

| $\omega \setminus \mathcal{H}$ | 0.1 | 1.0 | 10.0 |
|---|---|---|---|
| $\pi\ /\ (5T_p)$ | $S_1$ | $S_2$ | $S_3$ |
| $2\pi\ /T_p$ | $S_4$ | $S_5$ | $S_6$ |
| $20\pi\ /T_p$ | $S_7$ | $S_8$ | $S_9$ |

Table 1. Values of $\omega$ and $\mathcal{H}$ examined.

**Description of the simulations $S_1, S_2, \cdots, S_9$**

Figs. 3.2, 3.3, and 3.4 show $R(T)$ *vs.* $T$ for the "low frequency" simulation parameter values $S_1$, $S_2$, and $S_3$, respectively. In this set of simulations, the

period of the time variable part of the abyssal current is $P_\omega \simeq 170$ compared to the period of the unforced Mooney and Swaters solution shown in Fig. 3.1 given by $T_p \simeq 17$. Figs. 3.2, 3.3, and 3.4, respectively, have $\mathcal{H} = 0.1$, 1.0 and 10.0.

Clearly, comparing Figs. 3.2, 3.3, 3.4 with Fig. 3.1, there is marked change in the evolution in $R(T)$. However, there are some patterns that can be observed. The first thing to note is that the period of the oscillations in Figs. 3.2, 3.3, and 3.4 is smaller than that in Fig. 3.1 Further, comparing Fig. 3.2 with Fig. 3.3 and Fig. 3.4, we see that as $\mathcal{H}$ increases, so too does the frequency of the oscillations. Also, we see that, qualitatively, the "maximum" peak to trough distance, i.e., the *range* of $R(T)$, also seems to increase as $\mathcal{H}$ increases. Thus, in general, we see that, for this value of $\omega$, there is a trend toward more rapid oscillations with the range of $R(T)$ increasing.

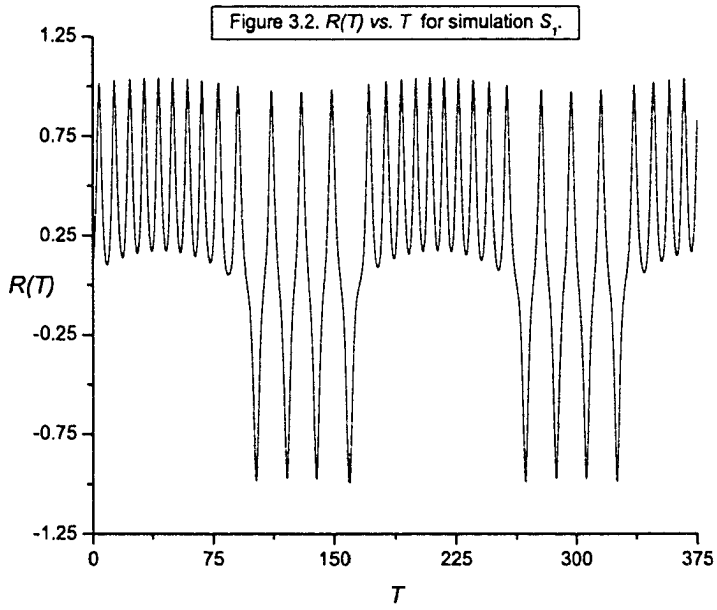

Nevertheless, we see in Figs. 3.2, 3.3, and 3.4, that, although the structure of $R(T)$ appears to be quite complicated, the solution appears to be periodic (at least for the range of $T$ we integrated over). In Fig. 3.2 the pattern appeared to follow 9 subcycles where $R(T)$ remained positive and then switched to a 4 subcycle pattern where the amplitude in $R(T)$ increased and $R(T)$ can become negative. The pattern then repeats itself. We note that when $R(T)$ goes negative, this corresponds to the underlying normal mode going 180° out of phase with the Mooney and Swaters (1996) solution.

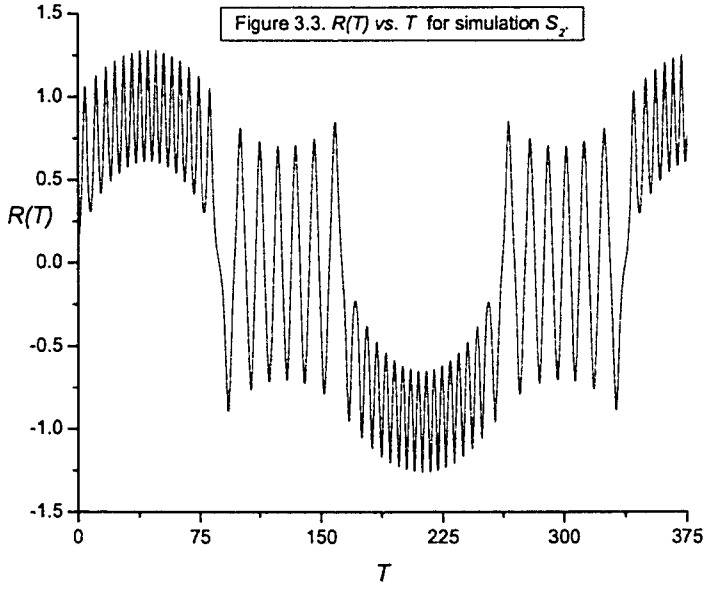

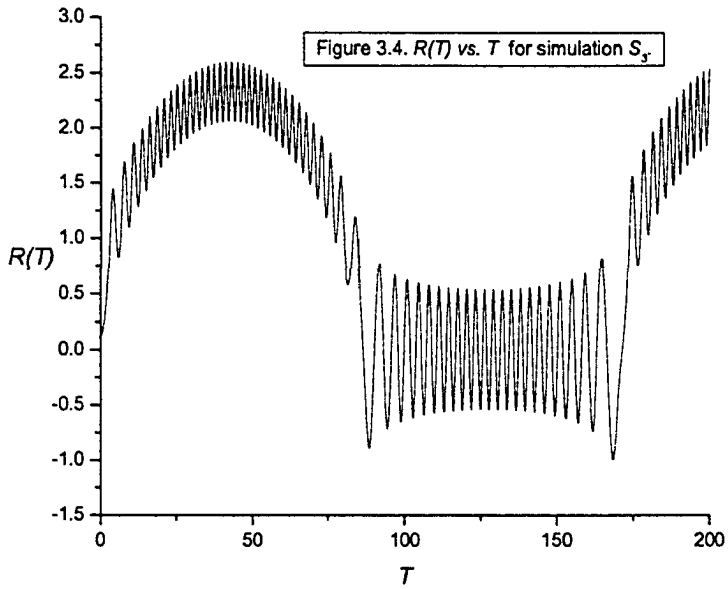


The pattern in Figs. 3.3 and 3.4 appears to be more complicated as compared to Fig. 3.2. But, qualitatively, there are similarities (and, of course, differences) in all three figures. We see that initially (i.e., $0 \leq T \leq T_*$) there is a set of cycles where the envelope of the oscillations is concave up and where $R(T) > 0$. The number of cycles in the region appears to increase with increasing $\mathcal{H}$. Subsequent to this set of initial cycles, there is a transition to a second set of cycles. In all three figures, this second set of cycles appears to oscillate about $R(T) \approx 0$. However, whereas in Figs. 3.2 and 3.4 there appears to be a transition back to the initial set of cycles from the second set, in Fig. 3.3, $R(T)$ transitions to a distinct third set of cycles from the second. However, again qualitatively, this third set of cycles in Fig. 3.4 appears to be a "reflection" of the first set of cycles through the $T$-axis.

Figs. 3.5, 3.6 and 3.7 show $R(T)$ *vs.* $T$ for the simulation parameter values $S_4$, $S_5$, and $S_6$, respectively. In this set of simulations, the period of the time

variable part of the abyssal current is $P_\omega = T_p \simeq 17$ (i.e., is comparable to the period of the unforced Mooney and Swaters solution shown in Fig. 3). Figs. 3.5, 3.6 and 3.7, respectively, have $\mathcal{H} = 0.1$, 1.0 and 10.0.

The structure of $R(T)$ in Figs. 3.5, 3.6 and 3.7 is different than that seen in Figs. 3.2, 3.3 and 3.4. Indeed, our numerical integrations suggested that there was no periodic structure at all. It is possible that there is a very long time scale periodic structure that we were not able to identify because we failed to integrate for a sufficiently long time. Nevertheless, although we have not identifies a global periodic structure, clearly, the solutions continue to exhibit quasi-periodic oscillatory behavior.

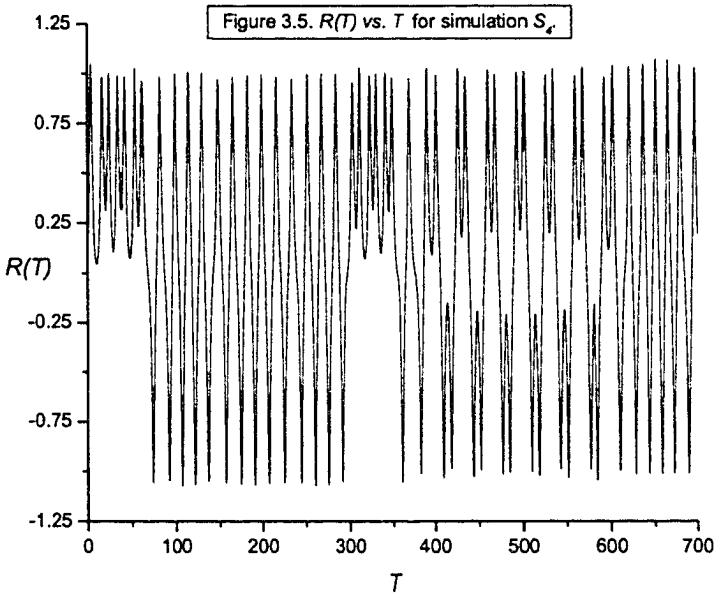

Figure 3.6. *R(T) vs. T* for simulation $S_5$.

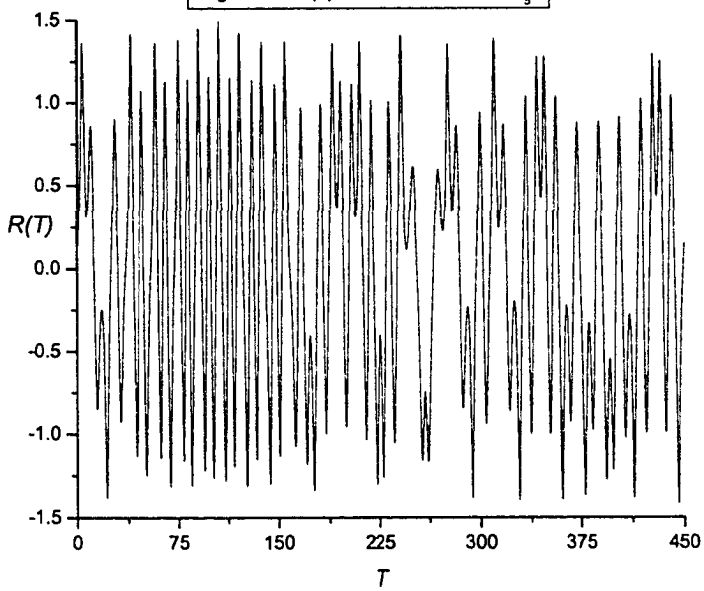


Figure 3.7. *R(T) vs. T* for simulation $S_6$.

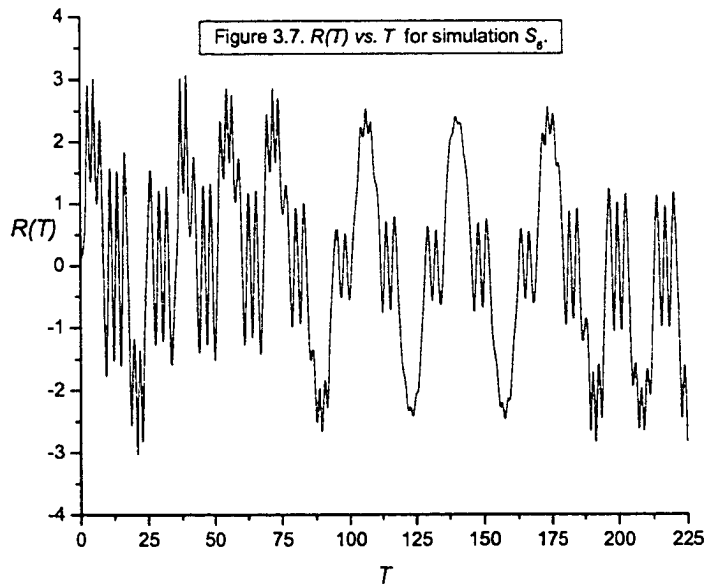

However, in Fig. 3.5 we see, again, the pattern that initially (i.e., $0 \leq T \leq T_*$) there is a set of cycles where $R(T) > 0$. Subsequent to this set of initial cycles, there is a transition to a second set of cycles that appears to oscillate about $R(T) \approx 0$. Subsequent to this second set of cycles, there is a transition to a third set of cycles that appears to be similar to the first set although there are fewer of them. Subsequent to this third set of cycles, there is a transition to a fourth set of cycles that appears to be similar to the second set but is clearly different. Continued numerical integration was unable to identify any periodicity.

In Figs. 3.6 and 3.7, we see the increasing irregularity emerging in the oscillations. In Figs. 3.6 and 3.7, there appears to be only one or two initial cycles where $R(T) > 0$ and then an almost immediate transition to a set of similarly structured cycles that appears to oscillate about $R(T) \approx 0$. But then there is a subsequent transition to a set of new cycles that appears to be increasingly irregular. This transition takes place sooner in Fig. 3.7 that in Fig. 3.6.

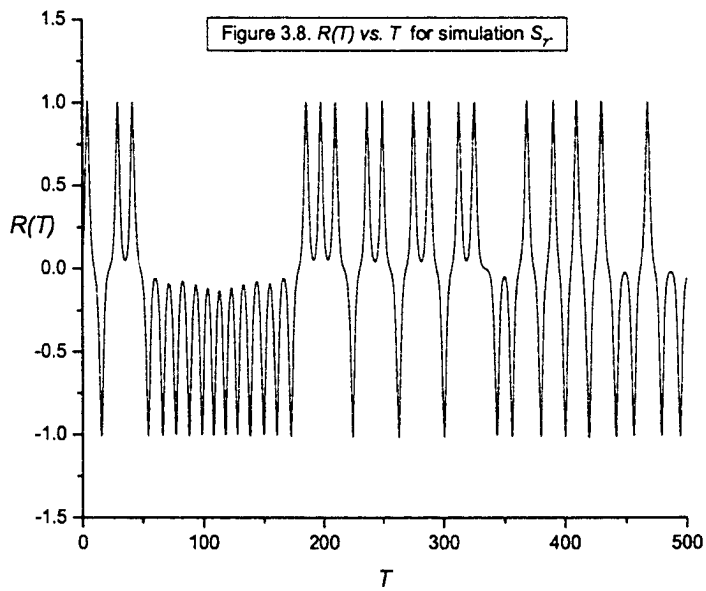

It is important to note, however, that this irregularity is not the onset of instability. The solutions remain bounded in time as they must. Although it is way beyond the scope of this thesis, it is interesting to speculate that the increasing irregularity seen in these simulations is an indication of chaos developing.

Figs. 3.8, 3.9 and 3.10 show $R(T)$ *vs.* $T$ for the "high frequency" simulation parameter values $S_7$, $S_8$, and $S_9$, respectively. In this set of simulations, the period of the time variable part of the abyssal current is $P_\omega \simeq 1.7$ compared to the period of the unforced Mooney and Swaters solution shown in Fig. 3 given by $T_p \simeq 17$. Figs. 3.8, 3.9 and 3.10, respectively, have $\mathcal{H} = 0.1$, 1.0 and 10.0.

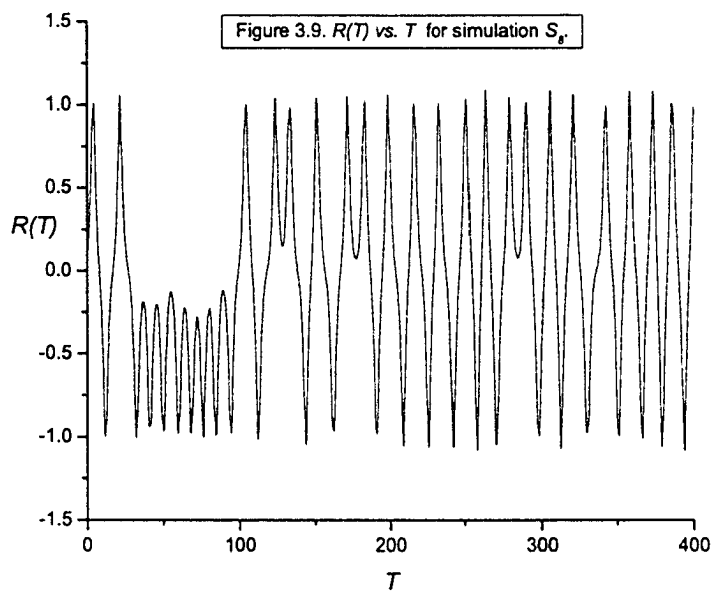

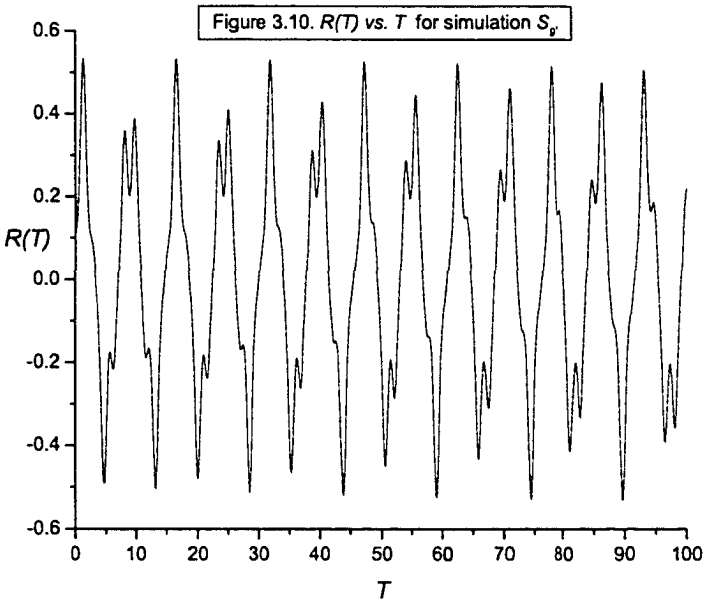


As in Figs. 3.5, 3.6 and 3.7, our numerical integration did not reveal any global periodicity in Figs. 3.8, 3.9 and 3.10 as well. However, qualitatively, it appears that the oscillation patterns seen in Figs. 3.8, 3.9 and 3.10 are somewhat less irregular than that seen in Figs. 3.5, 3.6 and 3.7. We attribute this to the fact that the periodicity in the time varying part of the abyssal current in Figs. 3.5, 3.6 and 3.7 is identical to the period of the Mooney and Swaters (1996) solution as seen in Fig. 3.1. It is possible that a nonlinear resonance exists in Figs. 3.5, 3.6 and 3.7 that does not occur in the other simulations and that this allows more "structure" to occur in the other figures.

### The evolution of $R(T)$ when $\Upsilon_0 = -1$ and $\Upsilon(T) \neq 0$

Even in the case where the underlying mode is subcritical (i.e., $\Upsilon_0 = -1$), we will show time variability can lead to instability if the nonlinear terms are neglected

in the amplitude equation. If we substitute $\Upsilon_0 = -1$ and

$$\Upsilon(T) = \mathcal{H}\cos(\omega T),$$

into (3.5.5), we obtain the nonlinear *Mathieu equation*

$$R_{TT} = \sigma^2 [\mathcal{H}\cos(\omega T) - 1] R - NR(R^2 - R_0^2). \tag{3.5.18}$$

Note, that this choice of $\Upsilon(T)$ allows the effect of time variability to be immediate at $T = 0$.

The first thing to note is that in the purely linear limit, i.e., $N = 0$, (3.5.18) reduces to the linear Mathieu equation

$$R_{TT} + \sigma^2 [1 - \mathcal{H}\cos(\omega T)] R = 0. \tag{3.5.19}$$

This equation has much more interesting stability properties (see, for example, Sec. 11.4 in Bender and Orszag, 1978) than the linear Mathieu equation derived in the last subsection. Note that if $\mathcal{H} = 0$, then the solutions to (3.5.19) simply oscillate in time reflecting, of course, the neutral stability of the underlying normal mode and, in fact, the solution to (3.5.18) subject to (3.5.6), is given by

$$R(T) = R_0 [\cos(\sigma T) + \sin(\sigma T)]. \tag{3.5.20}$$

In Fig. 3.11 we show a plot of $R(T)$ *vs.* $T$ for $R_0 = 0.1$ (implies that $R(0) = 0.1$ and $R_T(0) = \sigma/10$) with $\sigma = 1/\sqrt{2}$ (i.e., $k = l = 1.0$) as determined by (3.5.20). The solution is, of course, neutrally stable with a periodicity of about 8.886 units (with respect to $T$).

However, it is known (see, for example, Sec. 11.4 in Bender and Orszag, 1978) that, in the limit $\mathcal{H} \to 0$, the Mathieu equation (3.5.19) has unstable solutions (i.e., exponentially growing solutions) for the discrete frequency spectrum

$$\omega = 2\sigma/n, \text{ for } n = 1, 2, 3, \cdots. \tag{3.5.21}$$

For slightly larger $\mathcal{H}$ the discrete points for $\omega$ at which instability occurs expand into intervals of finite length, and as $\mathcal{H}$ gets even larger these intervals also get larger, so that eventually there is instability for almost all $\omega$. Accordingly, the generic situation associated with solutions to (3.5.18) is one of amplification. This process of destabilization, called "parametric instability," is the result of resonance developing between the underlying unforced periodic solution and the periodicity in $\Upsilon(T)$.

This is a very important result. We have therefore shown that in the linear limit, a periodic abyssal flow can lead to instability, even when the time mean average of the periodic flow is neutrally stable (provided that the frequency of the time varying part of the abyssal flow is algebraically related to the frequency of the neutrally stable normal mode associated with the time averaged abyssal flow as given by (3.5.21)).

In Fig. 3.12 we show a plot of $R(T)$ *vs.* $T$ for $R(0) = R_0 = 0.1$, $R_T(0) = \sigma R_0 = \sigma/10$ with $\sigma = 1/\sqrt{2}$ (i.e., $k = l = 1.0$; these are the same parameter values as those for Fig. 3.11) as determined by (3.5.19) with $\mathcal{H} = 0.25$ and $\omega = 2\sigma = \sqrt{2}$ (i.e., for $n = 1$ in (3.5.21)). The solution has been obtained numerically by using the routine *NDSolve* in the symbolic software package *Mathematica 4.0.* One can see the gradual amplification of the oscillations as $T$ increases. This increase in amplitude increases without bound. Higher values of $\omega$ and $\mathcal{H}$ act to increase the "growth rate" of the destabilization, but the basic pattern seen in Fig. 3.12 remains.

In Fig. 3.13 we show a plot of $R(T)$ *vs.* $T$ as determined by (3.5.18), for the same parameter values as that in Fig. 3.12, and additionally $N = 1.0$. One can see how the nonlinear terms act to stabilize the instability seen in Fig. 3.12. In addition, the nonlinear terms have acted to introduce a longer period modulation in the envelope of the amplitude.

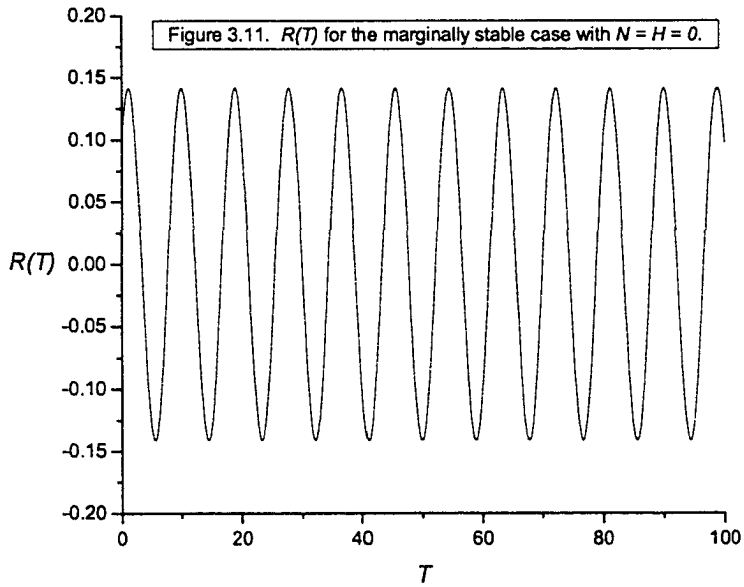


Figure 3.11. *R(T)* for the marginally stable case with $N = H = 0$.

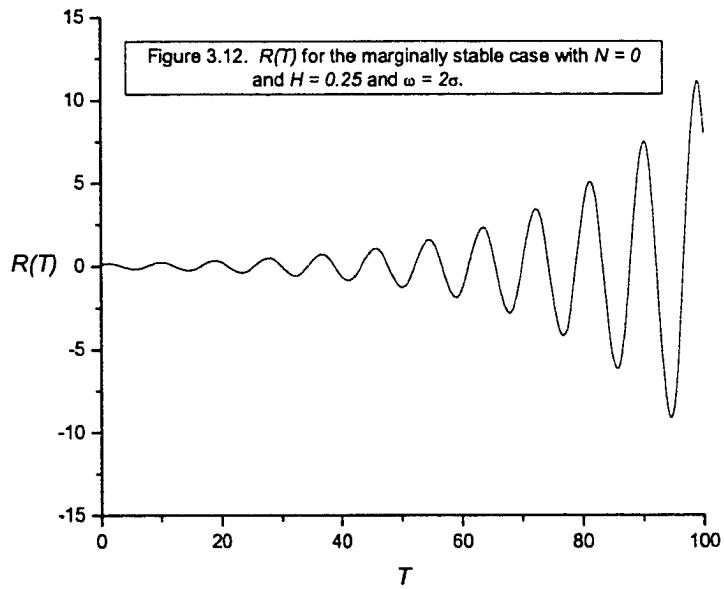


Figure 3.12. *R(T)* for the marginally stable case with $N = 0$ and $H = 0.25$ and $\omega = 2\sigma$.

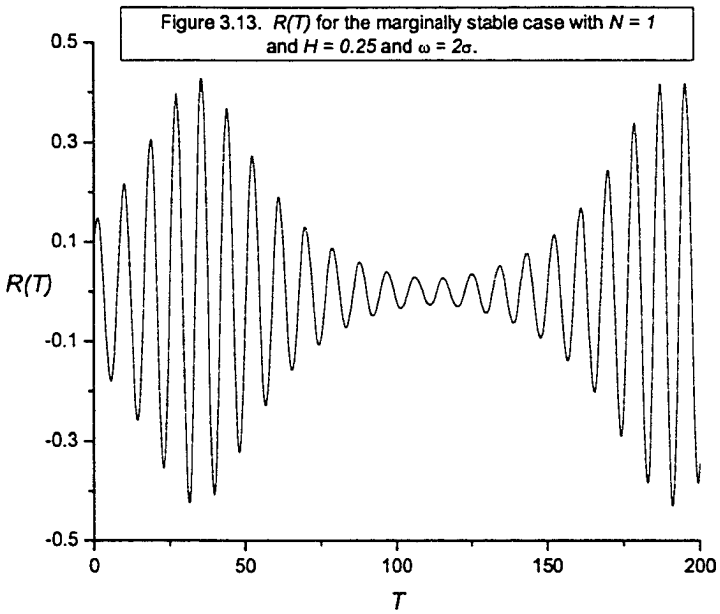


Figure 3.13. *R(T)* for the marginally stable case with $N = 1$ and $H = 0.25$ and $\omega = 2\sigma$.

# Chapter 4

# Weakly nonlinear evolution of a $K = 1$ unstable wave packet

In this Chapter, we examine the nonlinear development of a slightly supercritical $K = 1$ mode, which is the wavenumber modulus corresponding to the mode located at the minimum of the marginal stability curve (see Fig. 2.1) for which $\gamma_c = 0$. Under these conditions, a small but finite positive $\gamma$ will lead to a narrow band of unstable modes centered on $K = 1$. We wish to follow the evolution of the resulting baroclinic wave packet as it goes initially unstable and interacts with itself when the underlying abyssal current has periodic time variability.

The evolution of the marginally unstable $K = 1$ mode is singular in the sense that it cannot be described by simply taking the limit $K \to 1$, $\gamma_c \to 0$ and $c \to 1$ of the theory developed in Chapter 3 for the $K \neq 1$ modes. One immediate difference between the marginally unstable $K = 1$ and $K \neq 1$ modes which has significance follows from (3.2.7), where we see that the leading order amplitude in the abyssal layer satisfies $B \to 0$ in the limit $K \to 1$. This implies that the

leading order term $h_0(x, y, t, T) \equiv 0$ in the expansion (3.1.13) for $K \equiv 1$. This is equivalent to observing that, to leading order, the two layers are not dynamically coupled together for this marginally unstable mode.

However, this point alone is not sufficient to establish that the theory developed in Chapter 3 will not describe the finite amplitude evolution of a marginally unstable $K = 1$ mode. Indeed, if one takes the limit $K \to 1$, $\gamma_c \to 0$ and $c \to 1$ of the various coefficients in Chapter 3, it is easily seen that $\eta_0$, $\eta_1$, $h_0$ and $h_1$ all remain finite. The problem first arises in equation (3.4.11) for the $O(\varepsilon^2)$ problem where it is seen that $\eta_2$ and hence $h_2$ become singular in this limit. As we will show later in this Chapter, the problem can be traced to the fact that the theory developed for $h$ in Chapter 3 does not need to include the additional higher harmonics required in this section.

In addition, as we saw in Chapter 3, the phase velocity of the marginally unstable $K = 1$ mode will be given by $c = 1$ (see, e.g., (3.2.6)). This is nothing more than a reflection of the fact that, to leading order, it follows from (2.5.14) or (3.2.2) that the dynamics of the abyssal layer perturbation height is described by $h_t + h_x = 0$ in the weakly nonlinear marginally unstable limit at the point of marginal stability where $\gamma_c = 0$.

The fact that $c = 1$ means that the entire abyssal layer is a critical layer. Note that it follows from (2.5.4) that the leading order Eulerian velocity field in the abyssal layer is given by $\mathbf{u}_2 \simeq \widehat{\mathbf{e}}_1$. The steady velocity in the abyssal layer given by $\mathbf{u}_2 \simeq \widehat{\mathbf{e}}_1$, which we have previously referred to as the *Nof velocity*, arises due to the geostrophic adjustment of a density-driven abyssal flow lying directly on a sloping bottom. The phase speed of the marginally unstable $K = 1$ mode is therefore identical everywhere in the abyssal layer to the induced Nof velocity and the entire abyssal layer forms a critical layer. As is well known (see, e.g., Benney and Bergeron, 1969, or Warn and Gauthier, 1989), there will be a

rapid development of the dimensionality of the underlying phase space as more and more modes are excited by the fundamental harmonic due to the intrinsic nonlinearity of the critical layer.

From the point of view of the asymptotics, the nonlinear development of the marginally unstable $K = 1$ mode will, of course, be determined by the higher order, i.e., the nonlinear, terms in (2.5.12). However, since the leading order equation for $h$ is nondispersive, it necessarily follows that *all* the higher harmonics associated with the nonlinear terms in (2.5.12) will generate secular producing terms. These secular producing higher harmonics, which must be removed in a properly constructed asymptotic theory, lead inevitably to an infinity of wave packet evolution equations in sharp contrast to the single mode theory for the $K \neq 1$ modes developed in Chapter 3.

## 4.1 Developing the asymptotic expansion

In order to examine the nonlinear evolution of the marginally unstable $K = 1$ mode it is convenient to move into a co-moving reference frame in which the frequency, to leading order in the abyssal layer, will be zero. In this reference frame, the time development of the current height will be determined by the higher order, and importantly, the nonlinear Jacobian terms in (2.5.12).

To this end, and in light of the preceding comments, the correct scalings for the supercriticality in the slope of the abyssal height will be given by

$$\gamma = \varepsilon^2 \left[\Upsilon_0 + \Upsilon(T)\right], \; 0 < \varepsilon << 1, \; \Upsilon(T) \simeq O(1), \; \Upsilon_0 = \pm 1, \tag{4.1.1}$$

and the perturbation fields for the marginally unstable $K = 1$ and $\gamma_c = 0$ mode will scale according to

$$\eta(x, y, t) = \varepsilon \tilde{\eta}(\tilde{x}, y, X, T; \varepsilon), \tag{4.1.2}$$

$$h(x,y,t) = \varepsilon^2 \tilde{h}(\tilde{x}, y, X, T; \varepsilon). \tag{4.1.3}$$

with the fast space and slow space time variables given by, respectively,

$$\tilde{x} = x - t, \tag{4.1.4}$$

$$X = \varepsilon x, \; T = \varepsilon t, \tag{4.1.5}$$

so that derivatives map according to

$$\partial_t \rightarrow -\partial_{\tilde{x}} + \varepsilon \partial_T, \tag{4.1.6}$$

$$\partial_x \rightarrow \partial_{\tilde{x}} + \varepsilon \partial_X. \tag{4.1.7}$$

Substituting the above into the nonlinear perturbation equations (2.5.11) and (2.5.12) yields, after dropping the tildes and doing a little algebra,

$$(\Delta + 1)\eta_x = \varepsilon[\Delta \eta_T - 2\eta_{Xxx} - \eta_X - h_x + J(\eta, \Delta\eta)] + O(\varepsilon^2), \tag{4.1.8}$$

$$h_T + h_X - [\Upsilon_0 + \Upsilon(T)]\,\eta_x + J(\eta, h) = 0 + O(\varepsilon). \tag{4.1.9}$$

It is important to note the difference between the pair (4.1.8) and (4.1.9) and the pair (3.1.10) and (3.1.11). Although the upper layer equations (4.1.8) and (3.1.10) are both linear, to leading order, the abyssal layer equation (4.1.9) is fully nonlinear, to leading order, as compared to (3.1.11). This leading order nonlinearity is a consequence of the fact that the entire abyssal layer is a critical layer at the point of marginal stability given by $K = 1$ and $\gamma_c = 0$.

Following and extending Mooney and Swaters (1996), equations (4.1.8) and (4.1.9) can be approximately solved with an asymptotic expansion of the form

$$\eta(x,y,X,T;\varepsilon) = \eta_0(x,y,X,T) + \varepsilon\eta_1(x,y,X,T) + ..., \tag{4.1.10}$$

$$h(x,y,X,T;\varepsilon) = h_0(x,y,X,T) + \varepsilon h_1(x,y,X,T) + .... \tag{4.1.11}$$

Substitution of (4.1.10) and (4.1.11) into (4.1.8) and (4.1.9) gives rise to a sequence of partial differential equations that must be solved to obtain each term in the asymptotic sequence. As it turns out, the necessary analysis is both simpler and more complex than that developed in Chapter 3.

## 4.2 The $O(1)$ problem

The $O(1)$ equations are given by

$$(\Delta + 1)\eta_{0x} = 0, \tag{4.2.1}$$

$$h_{0T} + h_{0X} - [\Upsilon_0 + \Upsilon(T)]\,\eta_{0x} + J(\eta_0, h_0) = 0. \tag{4.2.2}$$

Note that the leading order equation for $\eta_0$ is not coupled to the abyssal layer equation. We may therefore solve (4.2.1) immediately to give

$$\eta_0 = A(X,T)\sin(ly)\exp(ikx) + c.c.. \tag{4.2.3}$$

Equation (4.2.2) *describes fully* the leading order evolution of $h_0(x, y, X, T)$. We need go no further in the asymptotic analysis of the abyssal layer equation. However to dynamically couple $\eta_0(x, y, X, T)$ with $h_0(x, y, X, T)$, that is, to determined the fully coupled evolution of $A(X,T)$ with $h_0(x, y, X, T)$, we need to examine the $O(\varepsilon)$ problem.

## 4.3 The $O(\varepsilon)$ problem

The $O(\varepsilon)$ upper layer equation is given by

$$(\Delta + 1)\eta_{1x} = \Delta\eta_{0T} - 2\eta_{0Xxx} - \eta_{0X} - h_{0x}, \tag{4.3.1}$$

where we have used $J(\eta_0, \Delta\eta_0) = 0$. We need to establish a solvability condition on (4.3.1) in order to remove secular growth in the $\eta_1$ solution.

The terms of on the right-hand side of (4.3.1) that will produce secular growth are those terms that are proportional to $\eta_0$, i.e., those proportional to $\sin(ly)\exp(\pm ikx)$. We may therefore write the solvability condition associated with (4.3.1) in the form

$$\int_0^L \int_0^{2\pi/k} [\Delta\eta_{0T} - 2\eta_{0Xxx} - \eta_{0X} - h_{0x}]\sin(ly)\exp(-ikx)\,dx\,dy = 0, \tag{4.3.2}$$

where the complex conjugate of this relationship is understood. Equation (4.3.2) is simply the geometric statement that the projection of the right-hand-side of (4.3.1) on the $\sin(ly)\exp(\pm ikx)$ mode must be zero.

Equations (4.2.2) and (4.3.2) (together with (4.2.3)) form a closed system of partial differential equations for $h_0(x, y; X, T)$ and $A(X, T)$. We have chosen to write the coupled equations in this way in order to emphasize the similarity with the analysis presented by Warn and Gauthier (1989) for a marginally unstable baroclinic flow in the Phillips' model.

As argued by Mooney and Swaters (1996), if one neglects the $\partial_X$ derivatives in (4.2.2) and (4.3.2) and assumes $\Upsilon(T) = 0$, it is possible to obtain a closed form solution in terms of elliptic and trigonometric functions by a slight modification of the methods presented in Warn and Gauthier (1989). We have not been able to generalize the Warn and Gauthier technique to the equations if one retains slow space variations in the wave amplitude or for nonzero $\Upsilon(T)$ and thus we construct a solution using the spectral approach developed by Mooney and Swaters (1996). We emphasize, however, that it remains an interesting and challenging problem to modify the Warn and Gauthier technique if one retains slow space variations in the wave amplitude or for nonzero $\Upsilon(T)$.

## 4.4 Spectral solution procedure

Here we construct an explicit spectral solution for $h_0$ in the form

$$h_0 = \phi(y, X, T) + \left\{ \sum_{m=1}^{\infty} \sum_{n=1}^{\infty} B_{m,n}(X, T) \sin(nly) \exp(imkx) + c.c. \right\}, \quad (4.4.1)$$

where $\phi(y, X, T)$ is a real valued mean flow adjustment term that will be determined as a result of the balance between the growth of the disturbance and the extraction of potential energy from the ambient flow.

If one substitutes (4.4.1) and (4.2.3) into (4.3.1) one obtains

$$(\Delta+1)\eta_{1x} = -ik\sum_{m=1}^{\infty}\sum_{n=1}^{\infty} mB_{m,n}\sin(nly)\exp(imk\theta)$$

$$-[\partial_T + (1-2k^2)\partial_X]A\sin(ly)\exp(ik\theta) + c.c. \qquad (4.4.2)$$

The only terms that cause resonant behavior on the left-hand side of (4.4.2) are those that are proportional to $\sin(ly)\exp(\pm ik\theta)$, which must be eliminated. Setting the coefficient of these terms to be equal to zero implies

$$ikB_{1,1} + A_T + (1-2k^2)A_X = 0, \qquad (4.4.3)$$

and, of course, its complex conjugate. Most importantly, however, is to note that (4.4.3) determines $B_{1,1}(X,T)$ as a function of $A(X,T)$. What remains to be done is to determine all the other $B_{m,n}(X,T)$, $A(X,T)$ and $\phi(y,X,T)$.

We proceed as follows. If one substitutes (4.4.2) and (4.2.3) into (4.2.2), one obtains

$$ik\left[\Upsilon_0 + \Upsilon(T) - \phi_y\right]A\sin(ly)\exp(ikx)$$

$$-\frac{1}{2}iklA\sum_{m=1}^{\infty}\sum_{n=1}^{\infty}\{nB_{m,n}\sin[(n+1)ly] - (n+1)B_{m,n+1}\sin(nly)$$

$$-mB_{m,n}\sin[(n+1)ly] - mB_{m,n+1}\sin(nly)\}\exp[i(m+1)kx]$$

$$+\frac{1}{2}iklA^*\sum_{m=1}^{\infty}\sum_{n=1}^{\infty}\{nB_{m,n}\sin[(n+1)ly] - (n+1)B_{m,n+1}\sin(nly)$$

$$+mB_{m,n}\sin[(n+1)ly] + mB_{m,n+1}\sin(nly)\}\exp[i(m-1)kx]$$

$$-\sum_{m=1}^{\infty}\sum_{n=1}^{\infty}(\partial_T+\partial_X)B_{m,n}\sin(nly)\exp(imkx) + c.c. - (\partial_T+\partial_X)\phi = 0. \qquad (4.4.4)$$

This expression is a double Fourier series in the orthogonal basis functions $\{\sin(nly)\}_{n=1}^{\infty}$ and $\{\exp(imkx)\}_{m=1}^{\infty}$. The evolution equations are obtained by demanding that each individual Fourier coefficient be identically zero.

To begin, the terms in (4.4.4) that are independent of the fast phase variable $x$ are given by

$$(\partial_T + \partial_X)\,\phi = \frac{1}{2} ikl A^* \sum_{n=1}^{\infty} \{ nB_{1,n} \sin[(n+1)ly] - (n+1)B_{1,n+1} \sin(nly)$$

$$+ B_{1,n} \sin[(n+1)ly] + B_{1,n+1} \sin(nly)\} + c.c. \tag{4.4.5}$$

Simplifying and including the complex conjugate explicitly, we find that

$$(\partial_T + \partial_X)\,\phi = \frac{1}{2} ikl \sum_{n=1}^{\infty} (n(AB^*_{1,n+1} - A^* B_{1,n+1})$$

$$-n(AB^*_{1,n-1} - A^* B_{1,n-1})) \sin(nly). \tag{4.4.6}$$

The solution to (4.4.6) may be written in the form

$$\phi\,(y, X, T) = \frac{1}{2} \sum_{n=1}^{\infty} \alpha_n(X, T) n \sin(nly). \tag{4.4.7}$$

Substituting (4.4.7) into (4.4.6) leads to the following set of equations for the $\alpha_n$ coefficients

$$(\partial_T + \partial_X)\,\alpha_n = ik[(AB^*_{1,n+1} - A^* B_{1,n+1}) - (AB^*_{1,n-1} - A^* B_{1,n-1})]. \tag{4.4.8}$$

Thus we have explicitly determined $\phi\,(y, X, T)$.

We now examine the $\exp(ikx)$ terms. The terms in (4.4.4) that are proportional to $\exp(ikx)$ are given by

$$ik\,[\Upsilon_0 + \Upsilon\,(T) - \phi_y]\,A \sin(ly)$$

$$+\frac{1}{2} ikl A^* \sum_{n=1}^{\infty} \{ nB_{2,n} \sin((n+1)ly) - (n+1)B_{2,n+1} \sin(nly)$$

$$+2B_{2,n} \sin((n+1)ly) + 2B_{2,n+1} \sin(nly)\}$$

$$- \sum_{n=1}^{\infty} (\partial_T + \partial_X)\, B_{1,n} \sin(nly) = 0. \tag{4.4.9}$$

If (4.4.7) is substituted into (4.1.25), we find, after some manipulation,

$$ikA\left[\Upsilon_0 + \Upsilon\left(T\right)\right] + ikAl^2\alpha_2 - \left(\partial_T + \partial_X\right)B_{1,1} = 0. \tag{4.4.10}$$

from the $\sin(ly)$ terms, and from the $\sin(nly)$ $(n > 1)$ terms

$$-\frac{1}{4}ikAl^2[\alpha_{n-1}(n-1)^2 + \alpha_{n+1}(n+1)^2]$$

$$+\frac{1}{2}iklA^*[(n+1)B_{2,n-1} - (n-1)B_{2,n+1}] - \left(\partial_T + \partial_X\right)B_{1,n} = 0, \tag{4.4.11}$$

and finally, the equations associated with the modes with $m > 1$ are given by

$$\left(\partial_T + \partial_X\right)B_{m,n} = \frac{1}{2}iklA^*[(n+m)B_{m+1,n-1} - (n-m)B_{m+1,n+1}]$$

$$-\frac{1}{2}iklA[(n-m)B_{m-1,n-1} - (n+m)B_{m-1,n+1}], \tag{4.4.12}$$

for $m = 2, 3, \ldots$, and $n = 1, 2, \ldots$ .

The entire set of coupled spectral equations can be cleaned up and consolidated if we introduce the transformations

$$\alpha_n = -\tilde{\alpha}_n, \; B_{m,n} = -i\tilde{B}_{m,n} \text{ (except for } B_{1,1}), \tag{4.4.13}$$

which yields the coupled set of partial differential equations

$$\left(\partial_T + \partial_X\right)[\partial_T + (1-2k^2)\partial_X]A = k^2\left[\Upsilon_0 + \Upsilon\left(T\right)\right]A - l^2k^2A\alpha_2, \tag{4.4.14}$$

$$\left(\partial_T + \partial_X\right)\alpha_2 = [\partial_T + (1-2k^2)\partial_X]\left|A\right|^2 + k[AB^*_{1,3} + A^*B_{1,3}], \tag{4.4.15}$$

$$\left(\partial_T + \partial_X\right)\alpha_n = k[AB^*_{1,n+1} + A^*B_{1,n+1} - (AB^*_{1,n-1} + A^*B_{1,n-1})], \tag{4.4.16}$$

for $n = 1, 3, 4, \cdots$, and

$$B_{1,1} = \frac{i}{k}\left[\partial_T + (1-2k^2)\partial_X\right]A, \tag{4.4.17}$$

$$\left(\partial_T + \partial_X\right)B_{m,n} = -\frac{1}{4}kAl^2[(n-1)^2\alpha_(n-1) - (n+1)^2\alpha_{n+1}]\delta_{1,m}$$

$$+\frac{1}{2}iklA^*[(n+m)B_{m+1,n-1} - (n-m)B_{m+1,n+1}]$$

$$-\frac{1}{2}iklA[(n-m)B_{m-1,n-1} - (n+m)B_{m-1,n+1}], \tag{4.4.18}$$

for $m, n = 1, 2, 3, \cdots$, except $m = n = 1$.

This set of equations is completely intractable so far as we know. Mooney and Swaters (1996) qualitatively examined these equations with $\Upsilon_0 = +1$ and $\Upsilon(T) = 0$. The method Mooney and Swaters (1996) used was to examine the evolution of the solution by truncating the spectral series after a certain number of terms. In particular they showed that if the cutoff was applied too soon after (but not directly after) a mean flow mode, then exponentially growing solutions resulted for $A(T)$. If the truncation was applied directly after a mean flow mode, then the equation set yielded bounded oscillating solutions, where the cycles forming a period became more complex with each increase in size of the set. This would seem to indicate that the mean flow modes have a stabilizing influence on the solutions, possibly by acting to restrict the potential energy available to the higher modes. We were unable to rigorously establish whether or not increasing the number of modes always leads to an increase in the number of cycles needed to form a period, although the numerical evidence seems to indicate this.

In terms of solutions that retain spatial variations, there is a soliton solution associated with the truncated model in which $B_{1,3}$ and all higher harmonics and the accompanying mean flows are ignored. In this limit, it is known (see Gibbon *et al.*, 1979) that this truncated model can be reduced to the *sine-Gordon* (*SG*) equation. The *SG* equation is a completely integrable nonlinear wave equation that has a soliton solution (Ablowitz and Segur, 1981). This soliton solution can be identified as an isolated abyssal wave packet that propagates nonlinearly and nondispersively in the along slope direction. Presumably, it is of interest to determine the propagation characteristics of the abyssal wave packet soliton solution, when the marginally unstable abyssal flow possesses time variability. This we do in the next Section.

## 4.5 Solution of the truncated soliton model with $\Upsilon(T) \neq 0$

If we neglect $B_{1,3}$ and all higher order terms, the truncated spectral equations are given by

$$(\partial_T + \partial_X)[A_T + (1-2k^2)A_X] = k^2\left[\Upsilon_0 + \Upsilon(T)\right]A - l^2k^2AB, \tag{4.5.1}$$

$$(\partial_T + \partial_X)B = \left[\partial_T + (1-2k^2)\partial_X\right]|A|^2, \tag{4.5.2}$$

where, for convenience, we have set $B \equiv \alpha_2(X,T)$. These equations are sometimes called the *AB equations*.

We note, immediately, that if one assumes that $\partial_X = 0$, this set of equations can be reduced to a single equation that is identical in form to the $K \neq 1$ amplitude equation (3.4.14). Thus, in this steady approximation of the truncated model, the effect of $\Upsilon(T) \neq 0$ on the evolution of $A(T)$ will be identical to that described in Chapter 3 and is not reproduced here. In this Section, we wish to focus on understanding the changes introduced into the propagation characteristics of the soliton solution to (4.5.1) and (4.5.2) by $\Upsilon(T)$.

To be concrete we will focus attention on the soliton solution associated with the marginally unstable situation with $\Upsilon_0 = +1$. There is a soliton solution associated with the marginally stable solution as well (the allowed sets of translation velocities associated with the marginally unstable and stable situations are disjoint from one another). The analysis is essentially the same and thus we do not include it here.

Our method of analysis is based on a nonlinear *WKB* procedure (Kodama and Ablowitz, 1980) developed for solitary waves that assumes that the time scale associated with $\Upsilon(T)$ is long in comparison to the advective time scale of

the solitary wave. We begin by assuming

$$\Upsilon_0 + \Upsilon(T) = 1 + \Upsilon(T) \equiv \gamma(\mu T), \tag{4.5.3}$$

where $\gamma(\mu T) \simeq O(1)$ and $0 < \mu << 1$, and that $A$ and $B$ are real valued and satisfy the far field conditions $|A, B| \to 0$ as $X \to \pm\infty$ for all $T \geq 0$. The solution to (4.5.1) and (4.5.2) is constructed in the form

$$A = A(\xi, \tau; \mu), \quad B = B(\xi, \tau; \mu), \tag{4.5.4}$$

where the new variables $(\xi, \tau)$ are given by

$$\xi = x - \frac{1}{\mu}\int_0^{\mu T} c(\zeta)\, d\zeta, \quad \tau = \mu T, \tag{4.5.5}$$

so that derivatives map according to

$$\partial_T = -c(\tau)\,\partial_\xi + \mu\partial_\tau, \ \partial_X = \partial_\xi,$$

where $c(\tau)$ is the soliton velocity.

Substitution of (4.5.4) and (4.5.5) into (4.5.1) and (4.5.2) leads to, after a little algebra,

$$[1 - c(\tau)]\left[1 - c(\tau) - 2k^2\right] A_{\xi\xi} - \gamma(\tau) A + k^2 l^2 AB =$$

$$-2\mu\left[1 - c(\tau) - k^2\right] A_{\xi\tau} + O\left(\mu^2\right), \tag{4.5.6}$$

$$[1 - c(\tau)]\, B_\xi - \left[1 - c(\tau) - 2k^2\right]\left(A^2\right)_\xi = \mu\left(A^2 - B\right)_\tau. \tag{4.5.7}$$

The solution to (4.5.6) and (4.5.7), in the limit of "small" $\mu$, can be found in the form

$$(A, B) = (A, B)^{(0)} + \mu(A, B)^{(1)} + \cdots. \tag{4.5.8}$$

Substitution of (4.5.8) into (4.5.6) and (4.5.7) leads to the following series of problems.

**The $O(1)$ problem**

The $O(1)$ equations are given by,

$$[1-c(\tau)]\left[1-c(\tau)-2k^2\right]A^{(0)}_{\xi\xi}-\gamma(\tau)A^{(0)}+k^2l^2A^{(0)}B^{(0)}=0, \tag{4.5.9}$$

$$[1-c(\tau)]B^{(0)}_{\xi}-\left[1-c(\tau)-2k^2\right]\left(\left[A^{(0)}\right]^2\right)_{\xi}=0. \tag{4.5.10}$$

Equation (4.5.10) can be integrated with respect to $\xi$, to yield

$$B^{(0)}=\frac{\left(1-c-2k^2\right)\left(A^{(0)}\right)^2}{(1-c)}, \tag{4.5.11}$$

which can be substituted into (4.5.9) to give

$$(1-c)\left(1-c-2k^2\right)A^{(0)}_{\xi\xi}-\gamma A^{(0)}+\frac{k^2l^2\left(1-c-2k^2\right)\left(A^{(0)}\right)^3}{(1-c)}=0. \tag{4.5.12}$$

It is straightforward to verify, by direct substitution, that (4.5.12) has the soliton solution

$$A^{(0)}(\xi,\tau)=A_0(\tau)\,\mathrm{sech}\left[\nu(\tau)\xi\right], \tag{4.5.13}$$

where

$$\nu(\tau)\equiv\sqrt{\frac{\gamma(\tau)}{[1-c(\tau)]\left[1-c(\tau)-2k^2\right]}}, \tag{4.5.14}$$

$$A_0(\tau)\equiv\sqrt{\frac{2\gamma(\tau)[1-c(\tau)]}{k^2l^2\left[1-c(\tau)-2k^2\right]}}, \tag{4.5.15}$$

which implies that $A_0$ and $\nu$ are related through the simple algebraic relation

$$A_0=\frac{\sqrt{2}(1-c)\nu}{kl}. \tag{4.5.16}$$

Thus given, $\gamma(\tau)$ and $c(\tau)$, the evolution of the soliton "wavenumber" $\nu(\tau)$ and amplitude $A_0(\tau)$ will be determined. The parameter $\gamma(\tau)$ is assumed known and $c(\tau)$ is determined by examining solvability conditions associated with the $O(\mu)$ problem.

Also, it follows from (4.5.14) and (4.5.15) that the product

$$[1-c(\tau)]\times\left[1-c(\tau)-2k^2\right],$$

has the same sign as $\gamma(\tau)$ or else $A_0$ and $\nu$ are not real valued, which is not allowed. Thus, if $\gamma(\tau)>0$, which corresponds to the marginally unstable case (that we examine here), then $c\in(-\infty,1-2k^2)\cup(1,\infty)$, and if $\gamma(\tau)<0$, which corresponds to the marginally stable case (that we do not examine here), then $c\in(1-2k^2,1)$.

### The $O(\mu)$ problem and the determination of $c(\tau)$

The $O(\mu)$ equations are given by

$$(1-c)\left(1-c-2k^2\right)A^{(1)}_{\xi\xi}-\gamma A^{(1)}+k^2l^2\left(A^{(0)}B^{(1)}+A^{(1)}B^{(0)}\right)=$$

$$-2\left(1-c-k^2\right)A^{(0)}_{\xi\tau}, \tag{4.5.17}$$

$$(1-c)\,B^{(1)}_{\xi}-2\left(1-c-2k^2\right)\left(A^{(0)}A^{(1)}\right)_{\xi}=\left(\left[A^{(0)}\right]^2-B^{(0)}\right)_{\tau}. \tag{4.5.18}$$

which are to be solved subject to the far field conditions $\left|A^{(1)},B^{(1)}\right|\to 0$ as $\xi\to\pm\infty$ for all $\tau\geq 0$.

The required solvability condition is that, considered as a $2\times 2$ system of ordinary differential equations (with respect to the variable $\xi$), the right hand side of (4.5.17) and (4.5.18) must be orthogonal to the kernel (i.e., the vector space spanned by the homogeneous solutions) of the adjoint system (see, for example, Kodama and Ablowitz, 1980 or Swaters and Flierl, 1991). The result of this solvability condition will be to derive an ordinary differential equation for $c(\tau)$.

When formulated this way, the solvability condition may be considered an application of the *Fredholm Alternative Theorem* (see, e.g., Boyce and DiPrima, 2005). In fact, the "removal of secular terms" procedure we used previously to

determine the amplitude equation for the marginally unstable (or stable) modes can also be seen as an application of the Fredholm Alternative Theorem in the situation where the operator associated with the homogeneous problem is self-adjoint or trivially non-self-adjoint.

We proceed as follows. We individually multiply (4.5.17) and (4.5.18) by the unknown test functions $\phi_1(\xi,\tau)$ and $\phi_2(\xi,\tau)$, respectively, integrate (by parts, repeatedly, where necessary) with respect to $\xi \in (-\infty,\infty)$, and add together. The result can be written in the form

$$\int_{-\infty}^{\infty} \left\{ A^{(1)} \left[ (1-c)\left(1-c-2k^2\right)\phi_{1\xi\xi} - \gamma\phi_1 + k^2 l^2 B^{(0)}\phi_1 \right.\right.$$

$$\left.\left. + 2\left(1-c-2k^2\right)A^{(0)}\phi_{2\xi} \right] + B^{(1)}\left[ k^2 l^2 A^{(0)}\phi_1 - (1-c)\phi_{2\xi} \right] \right\} d\xi =$$

$$-\int_{-\infty}^{\infty} \left\{ 2\left(1-c-k^2\right)\phi_1 A^{(0)}_{\xi\tau} + \phi_2 \left( \left[A^{(0)}\right]^2 - B^{(0)} \right)_\tau \right\} d\xi, \qquad (4.5.19)$$

where it is assumed that all the integrals exist.

The homogeneous adjoint problem associated with (4.5.17) and (4.5.18) is therefore given by

$$(1-c)\left(1-c-2k^2\right)\phi_{1\xi\xi} - \gamma\phi_1 + k^2 l^2 B^{(0)}\phi_1$$

$$+2\left(1-c-2k^2\right)A^{(0)}\phi_{2\xi} = 0, \qquad (4.5.20)$$

$$k^2 l^2 A^{(0)}\phi_1 - (1-c)\phi_{2\xi} = 0. \qquad (4.5.21)$$

If (4.5.11) and (4.5.21) is used to eliminate $B^{(0)}$ and $\phi_{2\xi}$, respectively, in (4.5.20), we obtain

$$(1-c)\left(1-c-2k^2\right)\phi_{1\xi\xi} - \gamma\phi_1 + \frac{3k^2 l^2 \left(1-c-2k^2\right)\left[A^{(0)}\right]^2}{(1-c)}\phi_1 = 0. \qquad (4.5.22)$$

Comparing (4.5.22) with (4.5.12) we see immediately that

$$\phi_1 = A^{(0)}_\xi, \qquad (4.5.23)$$

and, thus from (4.5.21), that

$$\phi_2 = \frac{k^2 l^2 \left[A^{(0)}\right]^2}{2(1-c)}. \tag{4.5.24}$$

Therefore, if (4.5.23) and (4.5.24) is substituted into (4.5.19), it follows that

$$\int_{-\infty}^{\infty} \left\{ 2\left(1-c-k^2\right) A_{\xi}^{(0)} A_{\xi\tau}^{(0)} \right.$$

$$\left. + \frac{k^2 l^2 \left[A^{(0)}\right]^2}{2(1-c)} \left( \left[A^{(0)}\right]^2 - B^{(0)} \right)_{\tau} \right\} d\xi = 0, \tag{4.5.25}$$

must hold. If (4.5.11) is used to eliminate $B^{(0)}$ in (4.5.25), the result can be written in the form, after a little algebra,

$$2\left(1-c-k^2\right) \frac{\partial}{\partial \tau} \left( \int_{-\infty}^{\infty} \left[A_{\xi}^{(0)}\right]^2 d\xi \right)$$

$$+ \frac{\partial}{\partial \tau} \left( \frac{k^4 l^2}{(1-c)^2} \int_{-\infty}^{\infty} \left[A^{(0)}\right]^4 d\xi \right) = 0. \tag{4.5.26}$$

If (4.5.13) is substituted into (4.5.26), the integrals are elementary to explicitly evaluate, and we obtain

$$\left(1-c-k^2\right) \left(\nu A_0^2\right)_{\tau} - k^4 l^2 \left[ \frac{A_0^4}{\nu (1-c)^2} \right]_{\tau} = 0,$$

and if (4.5.16) is substituted into this expression, the result can be written in the form

$$\left(1-c-3k^2\right) \left[(1-c)^2 \nu^3\right]_{\tau} = 0.$$

Generically,

$$c(\tau) \neq 1 - 3k^2 \text{ for all } \tau \geq 0,$$

so that we conclude

$$\left[(1-c)^2 \nu^3\right]_{\tau} = 0, \tag{4.5.27}$$

which can immediately be integrated to yield

$$\left[1-c(\tau)\right]^2 \nu^3(\tau) = (1-c_0)^2 \nu_0^3,$$

where $c_0 = c(0)$ and $\nu_0 = \nu(0)$, which if (4.5.14) is substituted in, implies,

$$\left\{\frac{\gamma(\tau)\sqrt[3]{[1-c(\tau)]}}{[1-c(\tau)-2k^2]}\right\}^{\frac{3}{2}} = \left\{\frac{\gamma_0\sqrt[3]{(1-c_0)}}{(1-c_0-2k^2)}\right\}^{\frac{3}{2}} \equiv \sqrt{\beta_0} > 0, \tag{4.5.28}$$

where $\gamma_0 = \gamma(0)$. It follows from (4.5.28) that $c(\tau)$ can be obtained by solving the cubic equation

$$\beta_0\left[1-c(\tau)-2k^2\right]^3 - \gamma^3(\tau)\left[1-c(\tau)\right] = 0. \tag{4.5.29}$$

Once $c(\tau)$ is determined, the result can be substituted into (4.5.14) and (4.5.15) to determine $\nu(\tau)$ and $A_0(\tau)$, which completes the determination of the leading order solution $A^{(0)}(\xi,\tau)$.

### An example calculation

We briefly describe an example calculation assuming that

$$\gamma(\tau) = 1 + \sin(\tau)/2, \tag{4.5.30}$$

i.e., the time variability is periodic with period $2\pi$ in units of $\tau$ with a range given by $\gamma(\tau) \in (0.5,\ 1.5)$. In addition, to be concrete, we assume that $k = l = 1/\sqrt{2}$ and that $c(0) = -2.0$. It follows from (4.5.14) and (4.5.16) that the initial soliton wavenumber and amplitude are given by $\nu(0) \simeq 0.41$ and $A_0(0) \simeq 3.46$, respectively. With the above choice of $\gamma(\tau)$, the abyssal current never goes subcritical and, thus, always remains supercritical.

With this choice of parameter values, (4.5.29) can be written in the form

$$c^3(\tau) - 8\gamma^3(\tau)c + 8\gamma^3(\tau) = 0, \tag{4.5.31}$$

since $\beta_0 = 3/8$. It follows from (4.5.31) that

$$c(\tau) = -\sqrt[3]{\frac{4}{3}}\gamma(\tau)\left[\sqrt[3]{1-\sqrt{1-\frac{32\gamma^3(\tau)}{81}}} + \sqrt[3]{1+\sqrt{1-\frac{32\gamma^3(\tau)}{81}}}\right], \tag{4.5.32}$$

It can be directly confirmed that $c(0) = -2$.

In Fig. 4.1 we plot the solution for the soliton velocity $c(\tau)$ as obtained from (4.3.32). The solution appears to be almost linearly proportional to $\gamma(\tau)$. However, this is not precisely true as the exact solution contains contributions from higher harmonics (i.e., the $32\gamma^3(\tau)/81$ terms) but these contributions have a small amplitude coefficient. In Figs. 4.2 and 4.3 we plot the solution for the soliton wavenumber $\nu(\tau)$ and amplitude $A_0(\tau)$, respectively, as obtained by substituting (4.3.32) into (4.5.14) and (4.5.15), respectively. As in Fig. 4.1, we see the almost linear proportionality with $\gamma(\tau)$.

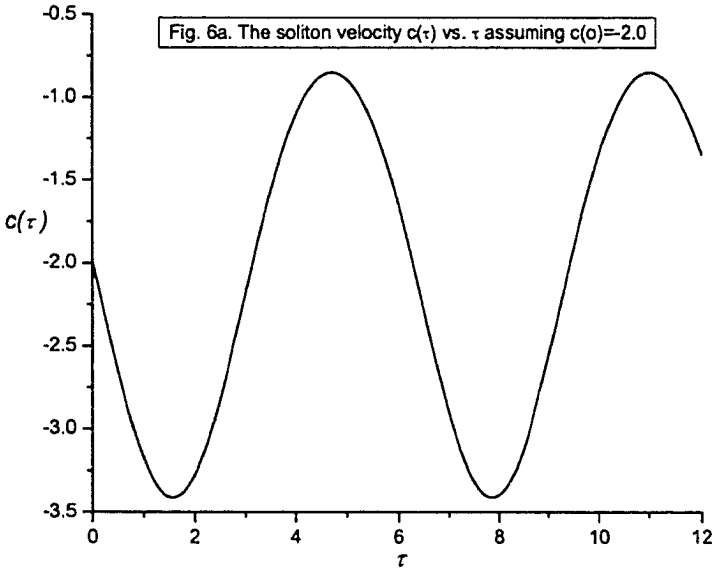

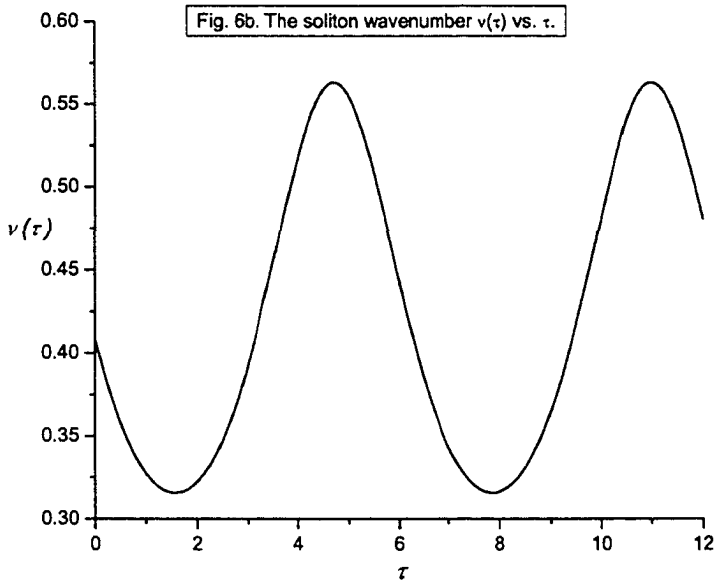


Fig. 6b. The soliton wavenumber $\nu(\tau)$ vs. $\tau$.

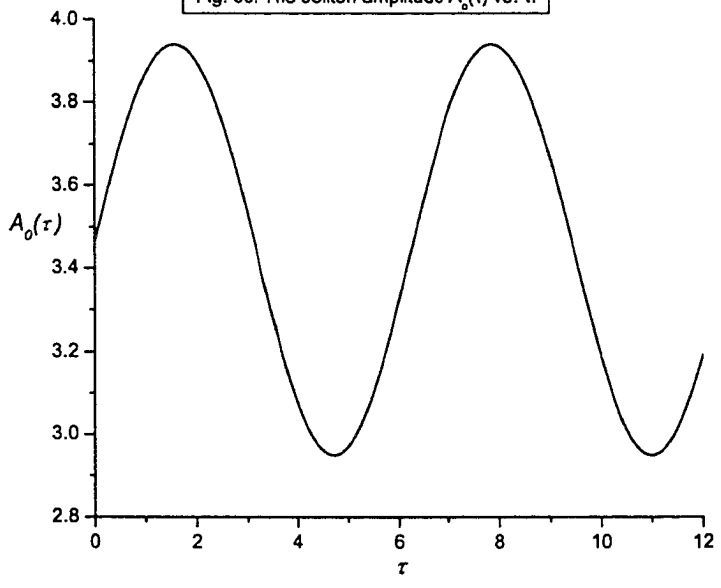


Fig. 6c. The soliton amplitude $A_o(\tau)$ vs. $\tau$.

# Chapter 5

# Summary and conclusions

A weakly nonlinear theory for a marginally stable or unstable, time-varying abyssal current has been studied. We extend the weakly nonlinear instability analysis of Mooney and Swaters (1996) to marginally stable or unstable, time-varying abyssal currents, using the methods described by Pedlosky and Thomson (2003). The governing equations originate from Swaters (1991) that describe the linear baroclinic instability of a grounded abyssal current on a sloping bottom. The model for this thesis is a two-layer system in which relatively dense water (the abyssal layer) sits directly on a sloping bottom surrounded by relatively lighter water (the upper layer).

We first derive the shallow water equations for each layer from the inviscid incompressible Navier-Stokes equations with constant density. The shallow water theory is based on a remarkable distinction between the horizontal and vertical length scales of geophysical fluid motion. We apply scalings to highlight the dynamics we expect to occur in the specific physical situation studied in this thesis. The Swaters (1991) model is obtained by an asymptotic reduction of the scaled model equations. Another way to derive the Swaters (1991) model is

presented by working from the potential vorticity equations for the full two layer shallow water equations.

We then continue to discuss the general linear, nonlinear stability theory and normal mode stability theory. Linear stability analysis is a procedure to examine the stability of the steady solution to small perturbations. We add a small perturbation term to the steady solution, substitute this into the nonlinear governing equations, and drop the nonlinear terms (the quadratic perturbation terms) to obtain the linear stability equations that describe the spatial structure and temporal evolution of the disturbances. Analyzing the energetics associated with destabilization gives us the fact that there must be at least one negative value of the slope of the abyssal height $h_0$ for instability to occur. When we consider a quadratically shaped abyssal height profile $h_0$ as shown in Fig. 1.1, which possesses two incroppings, a physical interpretation for this fact is that the instability occurs on the down slope side of the abyssal height ($h_{0y} \leq 0$). The normal mode linear instability equations are analyzed in order to generate a marginal stability curve. The marginal stability curve represents the boundary between stable and unstable modes for a particular cross-slope rate of change of the thickness of the abyssal current height versus the total wavenumber.

If there is instability in the linear stability analysis, the evolution of the wave always reaches amplitudes for which the linear theory is no longer valid. To see how the marginally unstable modes as determined by linear theory actually evolve in time we must develop a finite amplitude instability theory that describes the nonlinear interactions.

The case when the mode does not correspond to the point of marginal stability is examined first. We derive an amplitude evolution equation and solve for a weakly subcritical or supercritical abyssal flow with or without time variations. Without time variations, the amplitude evolution is periodic, which is determined

by Jacobi elliptic dnoidal function. When a periodic time variation is included, the normal mode amplitude satisfies a nonlinear Mathieu equation. When the nonlinear terms are neglected in the amplitude equation, i.e., the case of the linearized Mathieu equation, there exist periodic abyssal flow configurations that can stabilize an unstable abyssal flow. This situation occurs for an extremely small region in parameter space. The generic solution for this linearized Mathieu equation is not stable for most parameter values. We investigate the effect of adding the nonlinear term to this amplifying solution in time.

Nine different simulations are obtained by numerically integrating the amplitude equation, i.e., the nonlinear Mathieu equation with various amplitudes and periods of the time varying term. The three cases for the magnitude of the time varying term correspond to small, comparable, and large compared with the steady part of the supercriticality. The three cases for the period of the time varying term correspond to the periodicity being short, comparable and long, respectively, compared to the period of the disturbance without the time-varying terms. The amplitude functions are not periodic so that we allow sufficient length of time to confirm long time periods. When we have a low frequency parameter value of the time variable part of the abyssal current, there exist periodic abyssal flow configurations. For other ranges of frequency parameter values, the normal mode amplitude is no longer periodic and the pattern of the oscillation appears highly irregular. However, this irregularity is not the onset of instability because the normal mode amplitude still oscillates in time within a certain bound.

The second situation is that an amplitude evolution equation is in weakly subcritical modes. The solutions to the linearized Mathieu equation without the time-varying term are periodic. However, the linearized Mathieu equation including the time-varying term has unstable solutions. When we include the time-varying term into the Mathieu equation, the range of parameters that un-

stable solutions occur gets larger as the magnitude of time-varying term gets larger. We have therefore shown that in the linear limit, a stable and periodic abyssal flow can lead to instability. Numerical simulations show that the originally stable, periodic amplitude is amplified gradually as time goes by because of the effect of the time-varying term. However, there is a very interesting result about the presence of the nonlinear terms in the amplitude equation. The presence of the nonlinear terms in the amplitude equation always leads to the amplitude oscillating in time even though the amplitude is linearly unstable. We present a simulation that illustrates the periodic amplitude.

The evolution of modes that correspond to the point of marginal stability is singular because it cannot be described by taking the limit of the theory developed for the mode that do not correspond to the point of marginal stability. When the supercriticality is centred on the point of marginal stability, the weakly nonlinear instability theory for time varying abyssal flow generates fully a nonlinear partial differential equation for the unstable mode. Even at lowest order, there is an infinity of harmonics produced. The secular producing harmonics are removed by using asymptotic theory constructed properly. Based on a purely *ad hoc* basis, we choose only two truncated spectral equations which explain the fundamental mode and the mean flow it generates. The resulting equation set is equivalent to the *sine-Gordon* equation with time-dependent forcing. Without the forcing terms associated with the time dependent abyssal current, the truncated model has a soliton solution that can be identified as a steadily traveling coherent abyssal dome.

We develop an asymptotic expansion to describe the evolution of the abyssal soliton when the abyssal current is time varying. When we include the time-dependent periodic forcing term, the soliton amplitude is a smooth periodic function. This is a very important result. Initially unstable modes (the supercritical

modes) are stabilized by the time-dependent forcing for the wavenumber corresponding to the minimum of the marginal stability curve. We can compare this with the subcritical mode that the wavenumber modulus is not located at the minimum of the marginal stability curve. In this case, the amplitude is initially stable but the time variability of a periodic abyssal flow leads to instability.

The assumptions made for this thesis ignore many important physical configurations and dynamic processes such as separation and mixing by topography, and adiabatic and planetary effects. To understand the abyssal circulation occurring in the ocean, a theory including these features is necessary. It would be interesting to compensate the amplitude equation concerning realistic geophysical effects to understand an arbitrary shaped-abyssal current character. In view of extending the nonlinear regime of the marginal stability of the time-varying abyssal flow, applying other possible nonlinear terms would be another interesting topic to work on in the future.

# Bibliography


[1] Ablowitz, M. J., and H. Segur, 1981: *Solitons and the Inverse Scattering Transform*, SIAM Press, 425 pp.

[2] Bender, C. M., and S. A. Orszag, 1978: *Advanced Mathematical Methods for Scientists and Engineers*, McGraw-Hill, 593 pp.

[3] Benney, D. J., and R. F. Bergeron, R. F., 1969: A new class of nonlinear waves in parallel flows. *Stud. Appl. Math.* **48**, 181-204.

[4] Boyce, W. E., and R. C. DiPrima, 2005: *Elementary Differential Equations and Boundary Value Problems*, 8th Edition, Wiley, 790 pp.

[5] Bruce, J. G., 1995: Eddies southwest of Denmark Strait. *Deep-Sea Res.* **42**, 13-29.

[6] Choboter, P. F., and G. E. Swaters, 2000: On the baroclinic instability of axisymmetric rotating gravity currents with bottom slope. *J. Fluid Mech.* **408**, 149-177.

[7] Choboter, P. F., and G. E. Swaters, 2003: Two layer models of abyssal equator cross flow. *J. Phys. Oceanogr.* **33**, 1401-1415.

[8] Choboter, P. F., and G. E. Swaters, 2004: Shallow water modeling of Antarctic Bottom Water crossing the equator. *J. Geophys. Res.* **109**, C03038, doi:10.1029/2003JC002048.

[9] Drazin, P. G., and W. H. Reid, 1981: *Hydrodynamic Stability*, Cambridge University Press, 527 pp.

[10] Etling, D., F. Gelhardt, U. Schrader, F. Brennecke, G. Kühn, G. Chabert d'Hieres and H. Didelle, 2000: Experiments with density currents on a sloping bottom in a rotating fluid. *Dyn. Atmos. Oceans* **31**, 139-164.

[11] Gibbon, J. D., I. N. James, and I. M. Moroz, 1979: An example of soliton behavior in a rotating baroclinic fluid. *Proc. R. Soc. Lond.* **A 367**, 219-237.

[12] Gill, A. E., 1982: *Atmosphere-Ocean Dynamics*, Academic Press, 662 pp.

[13] Jiang, L., and R. W. Garwood Jr., 1996: Three dimensional simulations of overflows on continental slopes. *J. Phys. Oceanogr.* **26**, 1214-1233.

[14] Jungclaus, J. H., J. Hauser and R. H. Käse, 2001: Cyclogenesis in the Denmark Strait overflow plume. *J. Phys. Oceanogr.* **31**, 3214-3229.

[15] Karsten, R. H., and G. E. Swaters, 1996: Nonlinear stability of baroclinic fronts in a channel with variable topography. *Stud. Appl. Math.* **96**, 183-199.

[16] Karsten, R. H., G. E. Swaters and R. E. Thomson, 1995: Stability characteristics of Deep-Water Replacement in the Strait of Georgia. *J. Phys. Oceanogr.* **25**, 2391-2403.

[17] Kodama, Y., and M. J. Ablowitz, 1981: Perturbations of solitons and solitary waves. *Stud. Appl. Math.* **64**, 225-245.

[18] Kundu, P. K., 1990: *Fluid Mechanics*, Academic Press, 638 pp.

[19] LeBlond, P. H., H. Ma, F. Doherty, and S. Pond, 1991: Deep and intermediate water replacement in the Strait of Georgia. *J. Phys. Oceanogr.* **29**, 288-312.

[20] LeBlond, P. H., and L. A. Mysak, 1978: *Waves in the Ocean*, Elsevier, 602 pp.

[21] Masson, D., 2002: Deep water renewal in the Strait of Georgia. *Estuarine, Coastal and Shelf Science* **54**, 115-126.

[22] Mellor, G. L., 1996: *Introduction to Physical Oceanography*, AIP Press, 260 pp.

[23] Mooney, C. J., and G. E. Swaters, 1996: Finite amplitude baroclinic instability of a mesoscale gravity current in a channel. *Geophys. Astrophys. Fluid Dyn.* **82**, 173-205.

[24] Morse, P. M., and H. Feshbach, 1953: *Methods of Theoretical Physics*, McGraw-Hill, 1978 pp.

[25] Nof, D., 1983: The translation of isolated cold eddies on a sloping bottom. *Deep-Sea Res.* **30**, 171-182.

[26] Pavec, M., X. Carton and G. Swaters, 2004: Baroclinic instability of frontal geostrophic currents over a slope. *J. Phys. Oceanogr.*, in press.

[27] Pedlosky, J., 1970: Finite amplitude baroclinic waves. *J. Atmos. Sci.* **27**, 15-30.

[28] Pedlosky, J., 1972: Finite amplitude baroclinic wave packets. *J. Atmos. Sci.* **29**, 680-686.

[29] Pedlosky, J., 1982a: Finite amplitude baroclinic waves at minimum shear. *J. Atmos. Sci.* **39**, 555-562.

[30] Pedlosky, J., 1982b: A simple model for nonlinear critical layers in an unstable baroclinic wave. *J. Atmos. Sci.* **39**, 2119-2127.

[31] Pedlosky, J., 1987: *Geophysical Fluid Dynamics*, 2nd ed. Springer-Verlag, 710 pp.

[32] Pedlosky, J., 1996: *Ocean Circulation Theory*. Springer-Verlag, 453 pp.

[33] Pedlosky, J., and J. Thomson, 2003: Baroclinic instability of dependents currents. *J. Fluid Mech.* **490**, 189-215.

[34] Poulin, F. J., and G. E. Swaters, 1999a: Sub-inertial dynamics of density-driven flows in a continuously stratified fluid on a sloping bottom. I. Model derivation and stability conditions. *Proc. R. Soc. Lond. A* **455**, 2281-2304.

[35] Poulin, F. J., and G. E. Swaters, 1999b: Sub-inertial dynamics of density-driven flows in a continuously stratified fluid on a sloping bottom. II. Isolated eddies and radiating cold domes. *Proc. R. Soc. Lond. A* **455**, 2305-2329.

[36] Poulin, F. J., and G. E. Swaters, 1999c: Sub-inertial dynamics of density-driven flows in a continuously stratified fluid on a sloping bottom. Part 3. Nonlinear stability theory. *Can. Appl. Math. Quart.* **7**, 49-68.

[37] Reszka, M. K., G. E. Swaters and B. R. Sutherland, 2002: Instability of abyssal currents in a continuously stratified ocean with bottom topography. *J. Phys. Oceanogr.* **32**, 3528-3550.

[38] Smith, P. C., 1976: Baroclinic instability in the Denmark Strait overflow. *J. Phys. Oceanogr.* **6**, 355-371.

[39] Stommel, H., and A. B. Arons, 1960: On the abyssal circulation of the world ocean - I. Stationary flow patterns on a sphere. *Deep-Sea Res.* **6**, 140-154.

[40] Sutherland, B. R., J. Nault, K. Yewchuk and G. E. Swaters, 2004: Rotating dense currents on a slope. Part 1. Stability. *J. Fluid Mech.* **508**, 241-264.

[41] Swaters, G. E., 1991: On the baroclinic instability of cold-core coupled density fronts on sloping continental shelf. *J. Fluid Mech.* **224**, 361-382.

[42] Swaters, G. E., 1993: Nonlinear stability of intermediate baroclinic flow on a sloping bottom. *Proc. R. Soc. Lond. A* **442**, 249-272.

[43] Swaters, G. E., 1998: Numerical simulations of the baroclinic dynamics of density-driven coupled fronts and eddies on a sloping bottom. *J. Geophys. Res.* **103**, 2945-2961.

[44] Swaters, G. E., 2003: Baroclinic characteristics of frictionally destabilized abyssal overflows. *J. Fluid Mech.* **489**, 349-379.

[45] Swaters, G. E., and G. R. Flierl, 1991: Dynamics of ventilated coherent cold eddies on a sloping bottom. *J. Fluid Mech.* **223**, 565-587.

[46] Tan, B., and S. Liu, 1995: Collision interactions of solitons in a baroclinic atmosphere. *J. Atmos. Sci.* **52**, 1501-1512.

[47] Warn, T., and P. Gauthier, 1989: Potential vorticity mixing by marginally unstable waves at minimum shear. *Tellus* **41A**, 115-131.

[48] Warren, B. A., 1981: Deep circulation of the world oceans. In: *Evolution of Physical Oceanography.* Eds. Warren, B. A., and C. Wunsch. MIT Press, pp. 6-41..

[49] Whitehead, J. A., and L. U. Worthington, 1982: The flux and mixing rates of Antarctic Bottom Water within the North Atlantic. *J. Geophys. Res.* **87**, 7903-7924.

[50] Worthington, L. V., 1981: The water masses of the world ocean: some results of a fine scale census. In: *Evolution of Physical Oceanography.* Eds. Warren, B. A., and C. Wunsch. MIT Press, pp. 42-69.

[51] Wunsch, C., 1984: An eclectic Atlantic ocean circulation model. Part 1. The meridional flux of heat. *J. Phys. Oceanogr.* **14**, 1712-1733.

[52] Zoccolotti, L., and E. Salusti, 1987: Observations on a very dense marine water in the Southern Adriatic Sea," *Continent. Shelf Res.* **7**, 535-551.